

Synthesis, structural studies, and oxidation catalysis of the late first row transition metal complexes of a 2-pyridylmethyl pendant armed ethylene cross- bridged cyclam

*Donald G. Jones¹, Kevin R. Wilson¹, Desiray J. Cannon, Anthony D. Shircliff¹, Zhan Zhang²,
Zhuqi Chen², Timothy J. Prior^{3*}, Guochuan Yin^{2*}, Timothy J. Hubin^{1*}*

¹Department of Chemistry and Physics, Southwestern Oklahoma State University, 100 Campus Drive, Weatherford, OK 73096; ²Key Laboratory for Large-Format Battery Materials and System, Ministry of Education, School of Chemistry and Chemical Engineering, Hubei Key Laboratory of Material Chemistry and Service Failure, Huazhong University of Science and Technology, Wuhan 430074, PR China; ³Department of Chemistry, The University of Hull, Cottingham Road, Hull, UK, HU6 7RX.

KEYWORDS: cross-bridged cyclam, pendant-arm macrocycle, oxidation catalysis

ABSTRACT The first 2-pyridylmethyl pendant armed ethylene cross-bridged cyclam ligand has been synthesized and successfully complexed to Mn²⁺, Fe²⁺, Co²⁺, Ni²⁺, Cu²⁺, and Zn²⁺ cations. X-ray crystal structures were obtained for all six complexes and demonstrate pentadentate binding

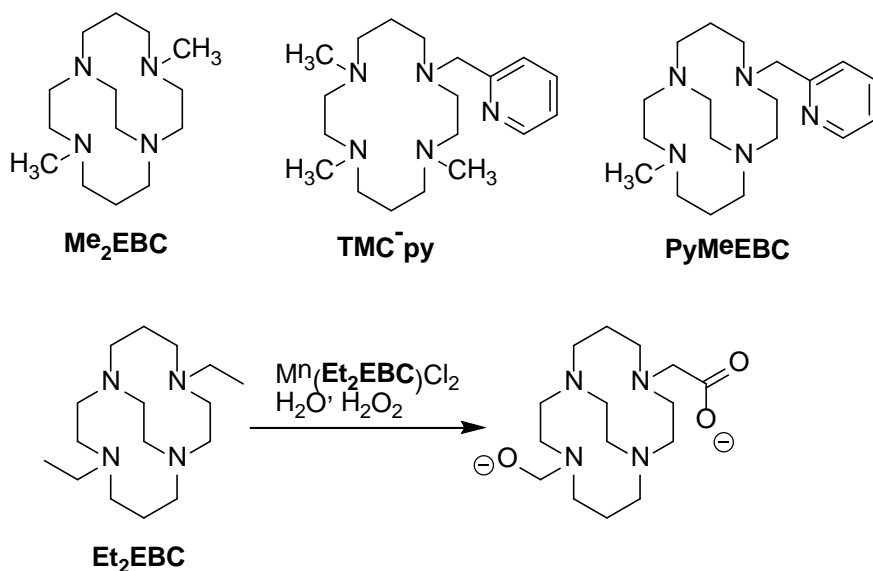
of the ligand with the requisite *cis-V* configuration of the cross-bridged cyclam ring in all cases, leaving a potential labile binding site *cis* to the pyridine donor for interaction of the complex with oxidants and/or substrates. The electronic properties of the complexes were evaluated using solid state magnetic moment determination and acetonitrile solution electronic spectroscopy, which both agree with the crystal structure determination of high spin divalent metal complexes in all cases. Cyclic voltammetry in acetonitrile revealed reversible redox processes in all but the Ni²⁺ complex, suggesting catalytic reactivity involving electron transfer processes are possible for complexes of this ligand. Kinetic studies of the dissociation of the ligand from the copper(II) complex under strongly acidic conditions and elevated temperatures revealed that the pyridine pendant arm actually destabilizes the complex compared to the parent cross-bridged cyclam complex. Screening for oxidation catalysis using hydrogen peroxide as the terminal oxidant for the most biologically relevant Mn²⁺, Fe²⁺, and Cu²⁺ complexes identified the Mn²⁺ complex as a potential mild oxidation catalyst worthy of continued development.

Introduction

Oxidation catalysis by cross-bridged cyclam complexes of manganese and iron has been studied for nearly a decade and a half. [1] [2] [3] [4] [5] [6] [7] [8] [9] [10] [11] [12] [13] [14] The manganese complex of 4,11-dimethyl-1,4,8,11-tetraazabicyclo[6.6.2]hexadecane [15] (**Me₂EBC**, **Scheme 1**) in particular, has a diverse and rich oxidation chemistry utilizing oxidation mechanisms ranging from hydrogen atom abstraction, electron transfer, concerted oxygen transfer, to the oxygen rebound mechanism. [5] [6] [7] [8] [9] [10] [11] [12] [13] [14] This compound, which we propose to call “the Busch catalyst”, was initially targeted as a potential oxidation catalyst because the rigid cross-bridged ligand could strongly bind the

oxygen-reactive manganese ion and prevent it from being deactivated in the form of MnO_2 . [1] [2] [3] [4] Additional critical ligand properties are thought to be the two available *cis* labile coordination sites for oxidant and substrate interaction, the methyl groups sterically preventing dimerization which might deactivate the catalyst, and the saturated and all-tertiary nitrogen nature of the ligand, which minimizes the possibility of ligand oxidation and catalyst destruction. [1] [2] [3] [4] $\text{Mn}(\text{Me}_2\text{EBC})\text{Cl}_2$ is a patented bleach catalyst heavily invested in by the laundry detergent industry because of its ability to activate $\text{O}_2/\text{H}_2\text{O}_2$ in water and remove stain molecules from cloth. [16] [17] [18] [19] [20] However, it has not been fully implemented in consumer products.

Scheme 1. Ligands discussed in this paper.



Recently, Que has revisited the iron complex of **Me₂EBC** and observed efficient olefin epoxidation catalysis with H_2O_2 oxidant under appropriate conditions. [21] In this study, it was shown that added acetic acid increases the yield of the epoxide product, and it was postulated that acetic acid binds to the iron center and facilitates O—O bond cleavage which is dependent

on the *cis* orientation of the two labile sites. Only one ligand-modified analogue of **Me₂EBC**, the diethyl analogue **Et₂EBC** (**Scheme 1**), has had its manganese complex oxidation catalysis explored. [22] [23] Interestingly, the seemingly simple exchange of methyl for ethyl groups results in a large change in catalyst oxidation potential and the surprising oxidation of the two ethyl groups into chelated methylene carboxylato and ethoxo groups (**Scheme 1**), respectively. While demonstrating the large possible effect of modifying the **Me₂EBC** ligand structure on oxidation potential and thus the resulting catalytic behavior, the hexadentate modified ligand product reduces the utility of the ultimate product in this case by coordinatively saturating it. Additional motivation derived from a trimethyl-pyridyl-cyclam (**TMC-py**, **Scheme 1**), having all but the desired ethylene cross-bridge of our preferred ligand characteristics (*vide supra*). Its iron complex activated dioxgen and formed an oxoiron(IV) intermediate that was crystallographically characterized, but has not been pursued further as a catalyst. [24] Although other pyridyl pendant armed unbridged cyclams are ubiquitous, [25] [26] [27] [28] [29] [30] [31] [32] [33] [34] [35] and a dipyridyl pendant armed cross-bridged cyclen has been published, [36] none of these ligands provide all of the desirable features for an oxidation catalyst (*vide supra*).

In this report, we offer our initial contribution to this field with the synthesis and characterization of a 2-pyridylmethyl N-pendant arm ethylene cross-bridged cyclam (**PyMeEBC**, **Scheme 1**) and its late first row transition metal (Mn²⁺, Fe²⁺, Co²⁺, Ni²⁺, Cu²⁺, and Zn²⁺) complexes. We chose to modify **Me₂EBC** by replacing only one methyl with a single 2-pyridylmethyl pendant arm, in order to maintain a labile non-chelated coordination site for interaction with oxidant/substrate. The additional aromatic nitrogen donor was expected to modify the steric and electronic properties of the metal ion, potentially as profoundly as the ethyl groups in **Et₂EBC**, [22] [23] resulting in modified oxidation chemistry. The pyridine pendant

would also maintain ligand neutrality and steric prevention of dimerization. It was furthermore expected that the quaternary, aromatic β -carbon of the pyridyl pendant arm would limit the reactivity of the ligand towards the oxidative modification found in **Et₂EBC**. Here, we disclose its synthesis; complexation to a range of late transition metals; the X-ray crystal structures of all six complexes; their electronic structure as revealed by magnetic moment, UV-Vis spectroscopy; cyclic voltammetry; and initial screening of the most biomimetically relevant complexes (manganese, iron, and copper) for the ability to catalyze oxidation reactions.

Important results and discussion include: (1) the synthesis of the first cross-bridged cyclam to include a pendant arm 2-pyridylmethyl group, which will no doubt be exploited by many other coordination chemists for a variety of purposes; (2) X-ray crystal structure characterization of a full series of first-row transition metal complexes from Mn through Zn in the same ligand giving an opportunity to examine coordination preference, and geometric and parametric changes as size and electronic properties change throughout the series; (3) the effect of an added pyridine donor on the electronic properties of the resulting complexes, most dramatically seen in the increased range of oxidation states available and increased reversibility observed in the cyclic voltammetry; (4) oxidation screening through hydrogen abstraction (HAT) and oxygen atom transfer reactions (OAT) that identify the Mn(**PyMeEBC**)Cl⁺ complex as an active oxidation catalyst that may have significant advantages over Mn(**Me₂EBC**)Cl₂ as a laundry bleach catalyst due to enhanced oxidation selectivity; and (5) kinetic decomplexation studies of the Cu(**PyMeEBC**)²⁺ complex that in comparison with literature data indicate that the pyridine pendant arm actually destabilizes the complex with respect to the parent **Me₂EBC** ligand, even though an additional chelate ring is added.

Experimental Section

General. N,N'-bis(aminopropyl)ethylenediamine (98%) and 2-picolyl chloride hydrochloride (98%), was purchased from Acros Organics. Glyoxal (40% wt in water), methyl iodide (99%), and sodium borohydride (98%), all anhydrous divalent transition metal chloride salts, and all anhydrous solvents used in the glovebox were purchased from Aldrich Chemical Co. All other solvents were of reagent grade and were used without modification. Cyclam was prepared according to a modified literature method from N,N'-bis(aminopropyl)ethylenediamine. [37] *cis*-3a,5a,8a,10a-tetraazaperhydropyrene (**1**) (cyclam glyoxal) was prepared according to a literature method. [38] Elemental analyses were performed by Quantitative Technologies Inc. Electrospray Mass spectra were collected on a Shimadzu LCMS-2020 instrument. All samples were dissolved in 50% H₂O/50%MeOH. NMR spectra were obtained on a Varian Bruker AVANCE II 300 MHz NMR Spectrometer. Electronic spectra were recorded using a Shimadzu UV-3600 UV-Vis-NIR Spectrophotometer. Magnetic moments were obtained on finely ground solid samples at ambient temperatures using a Johnson Matthey MSB Auto magnetic susceptibility balance.

Electrochemistry. Electrochemical experiments were performed on a BAS Epsilon EC-USB Electrochemical Analyzer. A button Pt electrode was used as the working electrode with a Pt-wire counter electrode and a Ag-wire pseudo-reference electrode. Scans were taken at 200 mV/s. Acetonitrile solutions of the complexes (1 mM) with tetrabutylammonium hexafluorophosphate (0.1 M) as a supporting electrolyte were used. The measured potentials were referenced to SHE using ferrocene (+0.400 V versus SHE) as an internal standard. All electrochemical measurements were carried out under N₂.

Acid Decomplexation Studies. [Cu(Me₂EBC)Cl]PF₆ synthesized according to the literature [39] and [Cu(PyMeEBC)][PF₆]₂ synthesized as below were used at 1 mM. The complex's lone

d-d absorption was recorded on a Shimadzu UV-3600 UV-Vis-NIR Spectrophotometer in 5 M HCl at both 90 °C and 50 °C over time. Typically, isosbestic spectra indicated only one decomposition product as the absorbance at λ_{max} decreased over time. Pseudo first-order conditions allowed the calculation of half-lives from the slopes of the linear $\ln(\text{absorbance})$ vs. time plots.

Synthesis

3a-(pyridin-2-ylmethyl)-decahydro-5a,8a,10a-triazaza-3a-azoniapyrenium iodide (2). 13.28 g (0.08096 mol, 2 eq.) of picolyl chloride hydrochloride and 13.60 g (0.1619 mol, 4 eq.) of anhydrous NaHCO₃ were stirred in 700 ml chloroform for 1 h. Solids were removed by filtration and the filtrate was added to 9.00 g (0.04048 mol, 1 eq.) of **(1)** and 13.44 g (0.08096 mol, 2 eq.) of KI. The reaction was stirred and heated to reflux for 6 d under nitrogen, during which it became an orange color. After cooling, minimal solids were removed by filtration and discarded. The filtrate was evaporated to 100 ml volume and excess diethyl ether was added to precipitate the yellow solid product, which was filtered on a glass frit, washed with diethyl ether, and dried under vacuum. Yield = 11.841 g (66%). Electrospray mass spectrometry gave a single peak at $m/z = 314$ corresponding to $(\text{M-I})^+$. Anal. Calc. for C₁₈H₂₈N₅I • H₂O: C 47.06, H 6.58, N 15.25; found: C 46.87, H 6.54, N 14.88. ¹H NMR (300 MHz, CDCl₃) δ 1.36 (d, 1H), 1.84 (d, 1H), 2.25 (m, 2H), 2.41 (d, 1H), 2.56 (d, 1H), 2.66 (m, 2H), 3.03 (m, 6H), 3.23 (t, 1H), 3.65 (m, 2H), 3.89 (d, 1H), 4.21 (m, 2H), 4.40 (td, 1H), 4.58 (s, 1H), 5.45 (m, 2H), 7.41 (m, 1H), 7.84 (m, 1H), 8.31 (d, 1H), 8.66 (d, 1H). ¹³C{¹H} NMR (75.6 MHz, D₂O) δ 18.0, 18.4, 41.9, 46.6, 49.4, 51.3, 51.9, 53.2, 54.0, 60.5, 62.9, 69.5, 82.2, 125.8, 129.0, 138.6, 146.6, 150.3.

3a-(pyridin-2-ylmethyl)-8a-methyl-decahydro-5a,10a-diaaza-3a,8a-diazoniapyrenium diiodide (**3**). 11.841 g (0.02683 mol, 1 eq.) of (**2**) was suspended in 690 ml of dry acetonitrile in a 1 L roundbottom flask. 15 eq (0.4025 mol, 57.13 g, 25.17 ml) of iodomethane was added, the flask was stoppered, and the reaction stirred at room temperature for 7 days. The light brown solid product was obtained by filtration on a glass frit, washing with diethyl ether, and drying under vacuum. A second crop was obtained by the addition of excess ether to the filtrate and was added to the first crop. Yield = 12.921 g (83%). Electrospray mass spectrometry gave peaks at $m/z = 456$ corresponding to $(M-I)^+$, $m/z = 328$ corresponding to $(M-2I)^+$, and $m/z = 165$ corresponding to $(M-2I)^{2+}$. Anal. Calc. for $C_{19}H_{31}N_5I_2 \cdot 0.5CH_3CN$: C 39.78, H 5.43, N 12.76; found: C 39.51, H 5.63, N 13.09. 1H NMR (300 MHz, $CDCl_3$) δ 1.80 (m, 2H), 1.97 (s, 3H), 2.32 (m, 3H), 2.79 (td, 1H), 3.10 (m, 5H), 3.38 (m, 5H), 3.55 (d, 2H), 3.72 (d, 2H), 4.51 (m, 2H), 5.18 (d, 2H), 7.52 (m, 1H), 7.65 (d, 1H), 7.93 (m, 1H), 8.65 (d, 1H). $^{13}C\{^1H\}$ NMR (75.6 MHz, D_2O) δ 17.1, 17.5, 45.3, 45.6, 47.4, 48.4, 48.7, 49.8, 50.2, 59.6, 62.0, 64.1, 73.6, 75.7, 125.0, 128.2, 137.7, 145.3, 149.5.

4-methyl-11-(pyridin-2-ylmethyl)-1,4,8,11-tetraazabicyclo[6.6.2]hexadecane (PyMeEBC). 9.010 g (0.0154 mol, 1 eq.) of (**3**) was dissolved in 550 ml of 95% EtOH. 8.739 g (0.2310 mol, 15 eq.) of sodium borohydride was added over 5 minutes. The reaction was then stirred under nitrogen for 5 days; copious white precipitate formed during the course of the reaction. Excess $NaBH_4$ was decomposed by the slow addition of concentrated HCl. The ethanol was removed under vacuum, after which 500 ml of 30% aqueous KOH was added. This basic solution was extracted with five 200 ml portions of benzene. The combined benzene layers were dried over sodium sulfate, filtered, and evaporated to a pale yellow oil which was not purified further. Yield = 4.550 g (89%). Electrospray mass spectrometry gave a single peak at $m/z = 332$

corresponding to $(\text{MH})^+$. Anal. Calc. for $\text{C}_{19}\text{H}_{33}\text{N}_5 \cdot 0.3 \text{H}_2\text{O} \cdot 0.1 \text{C}_6\text{H}_6$: C 68.29, H 10.00, N 20.32; found: C 68.40, H 10.52, N 20.33. ^1H NMR (300 MHz, CDCl_3) δ 1.68 (m, 4H), 2.30 (s, 3H), 2.85 (m, 18H), 3.58 (m, 4H), 7.16 (m, 2H), 7.61 (m, 1H), 8.49 (m, 1H). $^{13}\text{C}\{^1\text{H}\}$ NMR (75.6 MHz, CDCl_3) δ 22.9, 23.6, 41.5, 50.3, 50.6, 51.3, 51.8, 52.2, 52.8, 53.3, 55.7, 56.8, 57.6, 58.6, 122.0, 123.1, 135.6, 148.4, 156.1.

$[\text{Mn}(\text{PyMeEBC})\text{Cl}]\text{Cl}$: 1.000 g (0.003017 mol) of **(PyMeEBC)** and 0.380 g (0.003016 mol) anhydrous MnCl_2 were added to 20 ml of anhydrous acetonitrile in an inert atmosphere glovebox. The reaction was stirred at room temperature for 2 days during which the pink MnCl_2 beads dissolved and the white precipitate powder product precipitated. This product was obtained by filtration on a glass frit, washed with ether, and allowed to dry open to the atmosphere of the glovebox for four days. Yield = 0.930 g (67%). Electrospray mass spectrometry gave peaks at $m/z = 421$ corresponding to $(\text{Mn}(\text{PyMeEBC})\text{Cl})^+$ and $m/z = 193$ corresponding to $(\text{Mn}(\text{PyMeEBC}))^{2+}$. Anal. Calc. for $[\text{Mn}(\text{C}_{19}\text{H}_{33}\text{N}_5)\text{Cl}]\text{Cl} \cdot 0.1 \text{H}_2\text{O}$: C 49.70, H 7.29, N 15.25; found C 49.35, H 7.21, N 15.09.

$[\text{M}(\text{PyMeEBC})\text{Cl}]\text{PF}_6$ where $\text{M} = \text{Mn}^{2+}, \text{Fe}^{2+}, \text{Co}^{2+}, \text{Ni}^{2+},$ and Zn^{2+} : The general procedure for $[\text{Mn}(\text{PyMeEBC})\text{Cl}]\text{Cl}$ above was followed using 0.001 mol (0.332 g) of **PyMeEBC** and 0.001 mol of the respective anhydrous divalent metal chloride salt. [Because NiCl_2 has little solubility in acetonitrile, DMF was used as the solvent for this reaction only. The reaction was removed from the glove box and refluxed overnight before workup.] These reactions, other than Mn, gave little or no precipitation. All were filtered to remove trace solids, which were discarded (other than Mn which gave copious white solid, which was filtered, dissolved in minimum MeOH and precipitated with NH_4PF_6 as for the other metal ions). The filtrates were

then evaporated under vacuum to give crude $[M(\text{PyMeEBC})\text{Cl}]\text{Cl}$ solid products that were dissolved in a minimum MeOH in the glovebox. To each was added 0.815 g (0.005 mol, 5 eq.) of NH_4PF_6 likewise dissolved in a minimum of MeOH. Precipitation of the $[M(\text{PyMeEBC})\text{Cl}]\text{PF}_6$ products was immediate, but the suspensions were allowed to stir approximately 1 h to complete precipitation. The solid $[M(\text{PyMeEBC})\text{Cl}]\text{PF}_6$ products were filtered off, washed with diethyl ether, and allowed to dry overnight open to the glovebox atmosphere.

$[\text{Mn}(\text{PyMeEBC})\text{Cl}]\text{PF}_6$: Yield = 0.302 g (53%) of white powder. Electrospray mass spectrometry gave peaks at $m/z = 421$ corresponding to $(\text{Mn}(\text{PyMeEBC})\text{Cl})^+$ and $m/z = 193$ corresponding to $(\text{Mn}(\text{PyMeEBC}))^{2+}$. Anal. Calc. for $[\text{Mn}(\text{C}_{19}\text{H}_{33}\text{N}_5)\text{Cl}]\text{PF}_6 \cdot 0.5 \text{H}_2\text{O}$: C 39.63, H 5.95, N 12.16; found C 39.46, H 6.08, N 12.16. X-ray quality crystals were obtained from the slow diffusion of diethyl ether into an acetonitrile solution in the glovebox.

$[\text{Fe}(\text{PyMeEBC})\text{Cl}]\text{PF}_6$: Yield = 0.357 g (58%) of yellow powder. Electrospray mass spectrometry gave peaks at $m/z = 422$ corresponding to $(\text{Fe}(\text{PyMeEBC})\text{Cl})^+$ and $m/z = 194$ corresponding to $(\text{Fe}(\text{PyMeEBC}))^{2+}$. Anal. Calc. for $[\text{Fe}(\text{C}_{19}\text{H}_{33}\text{N}_5)\text{Cl}]\text{PF}_6 \cdot 0.3 \text{NH}_4\text{PF}_6$: C 37.01, H 5.59, N 12.04; found C 37.10, H 5.27, N 12.09. X-ray quality crystals were obtained from the slow evaporation of a MeOH solution in the glovebox.

$[\text{Co}(\text{PyMeEBC})\text{Cl}]\text{PF}_6$: Yield = 0.401 g (70%) of pink powder. Electrospray mass spectrometry gave peaks at $m/z = 425$ corresponding to $(\text{CoLCl})^+$ and $m/z = 195$ corresponding to $(\text{CoL})^{2+}$. Anal. Calc. for $[\text{Co}(\text{C}_{19}\text{H}_{33}\text{N}_5)\text{Cl}]\text{PF}_6$: C 39.98, H 5.83, N 12.27; found C 39.89, H 5.54, N 12.18. X-ray quality crystals were obtained from the slow diffusion of diethyl ether into an acetonitrile solution in the glovebox.

[Ni(**PyMeEBC**)Cl]PF₆: Yield = 0.345 g (60%) of a brown powder. Electrospray mass spectrometry gave peaks at m/z = 424 corresponding to (Ni(**PyMeEBC**)Cl)⁺, m/z = 408 corresponding to (NiL(H₂O)₂)⁺, and m/z = 195 corresponding to (Ni(**PyMeEBC**))²⁺. Anal. Calc. for [Ni(C₁₉H₃₃N₅)Cl]PF₆ • 0.2 NH₄PF₆ • 1.5 H₂O: C 36.21, H 5.89, N 11.56; found C 36.36, H 5.61, N 11.26. X-ray quality crystals were obtained from the slow diffusion of diethyl ether into a DMSO solution outside of the glovebox.

[Zn(**PyMeEBC**)Cl]PF₆: Yield = 0.577 g (73%) of a white powder. Electrospray mass spectrometry gave peaks at m/z = 430 corresponding to (Zn(**PyMeEBC**)Cl)⁺ and m/z = 198 corresponding to (Zn(**PyMeEBC**))²⁺. Anal. Calc. for [Zn(C₁₉H₃₃N₅)Cl]PF₆: C 39.53, H 5.76, N 12.13; found C 39.22, H 5.49, N 11.99. X-ray quality crystals were obtained from the slow evaporation of a nitromethane solution (form 2) and from the slow diffusion of diethyl ether into an acetonitrile solution (form 1), both outside of the glovebox.

[Cu(**PyMeEBC**)](PF₆)₂: This complex was synthesized following the general synthesis of [M(**PyMeEBC**)Cl]PF₆ above. However, no chloride is bound to the metal ion and two hexafluorophosphate anions are required. Yield = 0.302 g (44%) of a bright blue powder. Electrospray mass spectrometry gave a peak at m/z = 197 corresponding to (Cu(**PyMeEBC**))²⁺. Anal. Calc. for [Cu(C₁₉H₃₃N₅)](PF₆)₂: C 33.32, H 4.86, N 10.22; found C 32.96, H 4.65, N 10.11. X-ray quality crystals were obtained from the slow diffusion of diethyl ether into an acetonitrile solution outside the glovebox.

Crystal Structure Analysis Single crystal X-ray diffraction data were collected in series of ω -scans using a Stoe IPDS2 image plate diffractometer utilising monochromated Mo radiation ($\lambda = 0.71073 \text{ \AA}$). Standard procedures were employed for the integration and processing of the data

using X-RED. [40] Samples were coated in a thin film of perfluoropolyether oil and mounted at the tip of a glass fibre located on a goniometer. Data were collected from crystals held at 150 K in an Oxford Instruments nitrogen gas cryostream.

Crystal structures were solved using routine automatic direct methods implemented within SHELXS-97. [41] Completion of structures was achieved by performing least squares refinement against all unique F² values using SHELXL-97. [41] All non-H atoms were refined with anisotropic displacement parameters. Hydrogen atoms were placed using a riding model. Where the location of hydrogen atoms was obvious from difference Fourier maps, C-H bond lengths were refined subject to chemically sensible restraints.

Catalytic sulfide oxidation by complexes In 5 mL of dry acetonitrile containing 0.1 M thioanisole and 0.33 mM complex, 0.2 mL of 30% H₂O₂ was added to initialize the reaction. The reaction mixture was stirred in a water bath at 303 K for 6 h, and the product analysis was performed by GC using the internal standard method. A parallel experiment without catalyst was conducted as control.

Catalytic hydrogen abstraction by complexes In 3 mL of methanol/water (1;1, v/v) containing 0.05 M 1,4-cyclohexadiene and 1 mM complex, 0.02 mL of 30% H₂O₂ were added to initialize the reaction. The resulting reaction mixture was stirred in a water bath at 303 K for 4 h, and product analysis was conducted by GC using the internal standard method. A parallel experiment without catalyst was conducted as control.

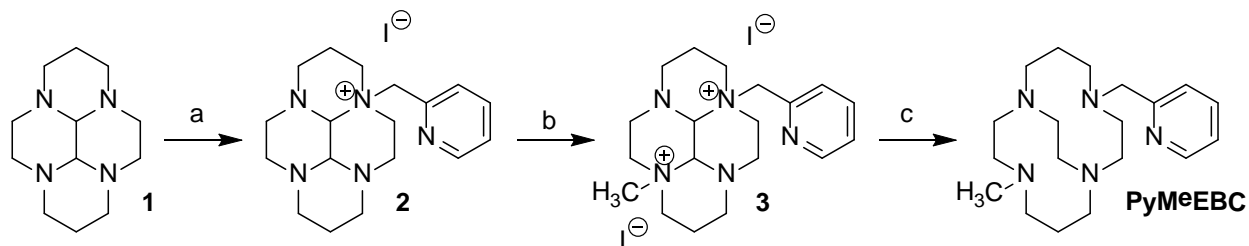
Results and Discussion

Synthesis

Attaching N-pendant 2-pyridylmethyl arms to ethylene cross-bridged tetraazamacrocycles would most efficiently be accomplished by reaction of a halomethylpyridyl moiety with a cyclam-glyoxal bisaminal following the teachings of Weisman [15] [42] [43] and Handel. [38] Initial attempts with picolyl chloride under the typical acetonitrile conditions for such reactions resulted in unsatisfactory red colored products where the color appeared due to reaction of the picolyl group with itself rather than the bisaminal. Literature investigation of the reactivity of halomethylpyridines and halomethylpyrazines led to work where these compounds were stabilized by storage in nonpolar chlorinated solvents. [44] Unsuccessful at alkylation of the bisaminals in typical S_N2 solvents like acetonitrile, we explored the chlorinated solvents and found successful, although low- yielding monoalkylation of the bisaminal **1** with picolyl chloride in chloroform at room temperature. It should be pointed out that others have alkylated cyclam-glyoxal condensates successfully in chloroform, as well. [45] Although we had apparently succeeded in retarding the self-reaction of the picolyl chloride, since little of the characteristic red color was produced and pure product was obtained, the yields were disappointing at ~10%. We were systematically able to raise the yields through activation of the electrophile by addition of KI to the reaction, although stoichiometric amounts were required. Additional increases in temperature (to reflux) and time (to 6 days) eventually led to respectable yields of the monoalkyl salt **2** (66% based on bisaminal **1**). Again, use of I⁻ [46] and heat [45] to increase reactivity of alkyl agents with macrocycle-glyoxal condensates are known strategies. Methylation of the non-adjacent nitrogen to produce **3** and NaBH₄ ring opening reduction to produce **PyMeEBC** successfully followed Weisman's typical procedures. [15] [42] [43]

Scheme 2. Synthesis of **PyMeEBC**. a) i. CHCl₃, 2 eq. picolyl chloride hydrochloride, 4 eq. NaHCO₃, 1 h, filter to remove solids; ii. 1 eq. of (**1**), 2 eq. KI, reflux 6 d; 66% yield b) CH₃CN,

15 eq. CH_3I , 7 d, rt; 83% yield c) i. 95% EtOH, 15 eq. NaBH_4 , N_2 , 5 d, rt; ii. 12 M $\text{HCl}(\text{aq})$, 30% $\text{KOH}(\text{aq})$, benzene extraction; 89% yield.



Complexation of **PyMeEBC** was carried out in acetonitrile (or DMF for acetonitrile-insoluble NiCl_2) with anhydrous divalent metal salts in an inert atmosphere glovebox. The white powder manganese complex $[\text{Mn}(\text{PyMeEBC})\text{Cl}]\text{Cl}$ precipitated from the reaction and was obtained in pure form by filtration. The other complexes were more soluble, so only trace solids were filtered off and the solvent evaporated. The crude chloride salts were not pure, so they were redissolved in methanol and the chloride anion replaced by addition of NH_4PF_6 to precipitate the pure $[\text{M}(\text{PyMeEBC})\text{Cl}]\text{PF}_6$ powder products. An exception to this formulation was the copper(II) complex, which remained 5-coordinate with no chloro ligand and precipitated as $[\text{Cu}(\text{PyMeEBC})][\text{PF}_6]_2$. To aid in crystallization, anion metathesis was similarly achieved to produce $[\text{Mn}(\text{PyMeEBC})\text{Cl}]\text{PF}_6$.

Complexation by cross-bridged tetraazamacrocycles is sometimes difficult, requiring heat or long reactions times. [4] Comparatively, complexation with **PyMeEBC** appeared qualitatively to be faster than usual in most cases. For example, crude $[\text{Mn}(\text{PyMeEBC})\text{Cl}]\text{Cl}$ white powder began to precipitate from the room temperature acetonitrile complexation solution within minutes. Similarly, the dramatic color changes indicating Cu^{2+} (dark blue-green) and Co^{2+} (dark purple) coordination with similar ligands were observed immediately upon addition of the metal

chloride salts to the room temperature acetonitrile ligand solutions. Therefore, no heat was added to any of the complexation reaction except for the NiCl₂ complexation, which was done in DMF to aid solubility of the NiCl₂ which required heat to fully dissolve this sparingly soluble salt fully. Certain pendant arms have been noted to aid the speed of complexation of tetraazamacrocycles, [47] [48] [49] [50] and it is possible that the pyridine pendant arm plays such a role here.

X-ray Crystal Structures

[M(PyMeEBC)Cl]PF₆ (M = Mn, Fe, or Co)

The M^{II} complexes [M(PyMeEBC)Cl]PF₆ (M = Mn, Fe, or Co) are isostructural and crystallize in the non-centrosymmetric space group Pca2₁. The unit cell volume decreases across this series from Mn to Co in line with the reduction in the metal ion radius. The Mn structure is representative of the others and that one will be discussed in detail to represent the set.

The metal ion lies in an approximately octahedral pocket, coordinated by one chloride anion and five nitrogen atoms from the ligand. The four nitrogen atoms from the macrocycle coordinate to the metal in an ‘all-*cis*’ arrangement with the pyridyl nitrogen of the pendant arm and the chloride also in a *cis* arrangement. (See **Figure 1**) This coordination is akin to the *cis-V* coordination displayed by tetra-azamacrocycles bound to a metal bearing two chloride anions. [1] [51] Although the four nitrogen atoms of the macrocycle bind to the metal with 4- and 5-membered chelate rings and N-Mn-N bite angles around 80° and 88°, respectively, the 4-membered chelating ring involving the pyridine is noticeably strained, with an N-Mn-N bite angle of 76.79(9)°.

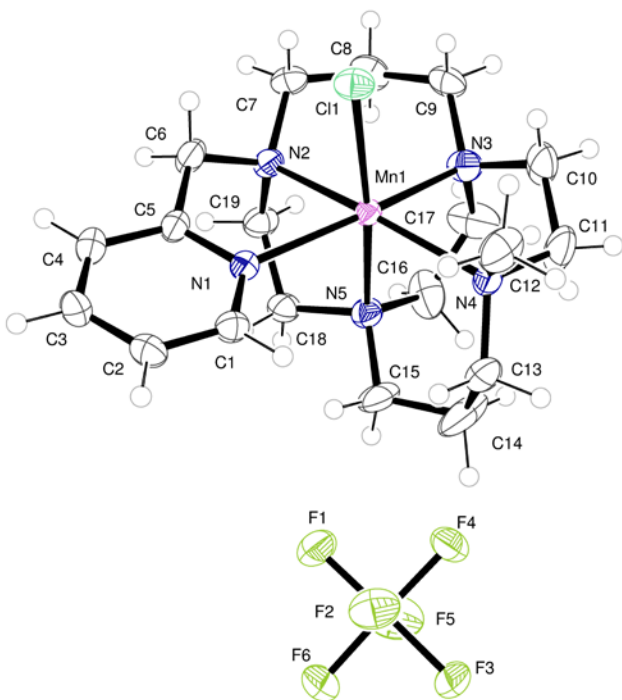


Figure 1. Asymmetric unit of $[\text{Mn}(\text{PyMeEBC})\text{Cl}]\text{PF}_6$ with atoms drawn as 50% probability ellipsoids. Atom colors: Mn pink; Cl green; C gray; N blue; F yellow-green.

$[\text{M}(\text{PyMeEBC})\text{Cl}]\text{PF}_6$ (M = Ni or Zn)

This macrocycle has also been shown to be a good ligand to smaller metal ions in the complex $[\text{Ni}(\text{PyMeEBC})\text{Cl}]\text{PF}_6$ and two different compounds containing the complex ion $[\text{Zn}(\text{PyMeEBC})\text{Cl}]\text{PF}_6$, hereafter labelled **Zn-1** (from diffusion of Et_2O into a CH_3NO_2 solution) and **Zn-2** (from evaporation of CH_3NO_2). The nickel compound is isostructural with **Zn-1**. Therefore, only the nickel compound and not **Zn-1** is described in detail, although the structural discussion applies equally for **Zn-1**.

Although this is centrosymmetric, the asymmetric unit features two symmetry-unique metal complexes, $[\text{Ni}(\text{PyMeEBC})\text{Cl}]^+$. They are each six coordinate but differ in the arrangement of the alkyl backbone of the ligand.

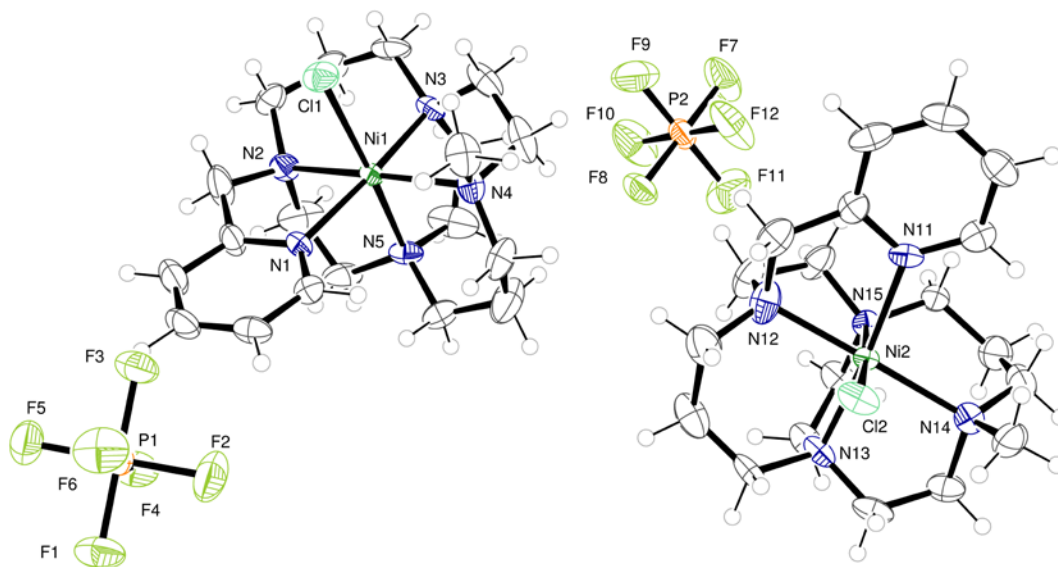


Figure 2. ORTEP representation of the asymmetric unit of $[\text{NiLCl}]\text{PF}_6$ with atoms drawn as 50% probability ellipsoids. Selected atoms are labelled. Atom colors: Ni deep green; Cl pale green; C gray; N blue; P orange; F yellow-green.

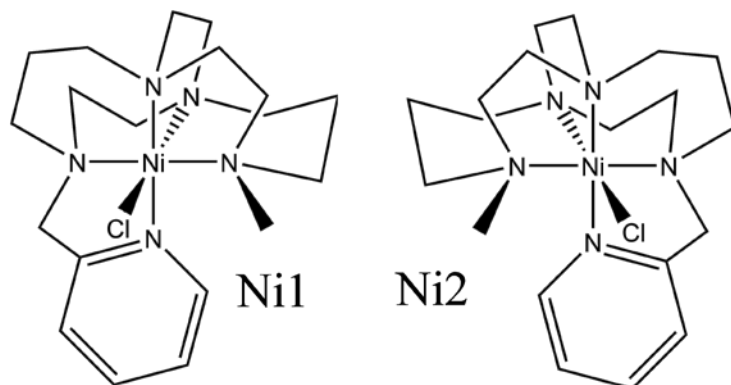


Figure 3. Representation of the coordination about the two symmetry unique metal ions in $[\text{Ni}(\text{PyMeEBC})\text{Cl}]\text{PF}_6$.

Figure 2 shows the crystallographic asymmetric unit and the geometry about the metal ion is each is further illustrated in **Figure 3**. The coordination about the nickel is completed by one chloride ion and five nitrogen atoms of the ligand. The two symmetry-unique metal ions display the same basic coordination but they are, effectively, although not crystallographically or even parametrically, mirror images. Essentially, the ligand can bind in right-handed or left-handed orientations, and each are separately present in Ni1 and Ni2. The N-Ni-N bite angles for the pendant pyridyl arm are $81.15(12)^\circ$ and $81.38(14)^\circ$ in the two complexes, suggesting a better fit of the Ni^{2+} ion to the macrocycle than for the larger Mn^{2+} .

The second polymorph of $[\text{Zn}(\text{PyMeEBC})\text{Cl}]\text{PF}_6$ contains a single, octahedrally coordinated Zn^{2+} ion in the asymmetric unit. The zinc ion is bound by five nitrogen atoms of the ligand and one chloride ion as shown in **Figure 4**. The coordination geometry is very similar to that of Ni1 in $[\text{Ni}(\text{PyMeEBC})\text{Cl}]\text{PF}_6$ (and hence Zn1 in **Zn-1**). The center of inversion within the structure means that the second enantiomer (akin to Ni2) is generated by symmetry.

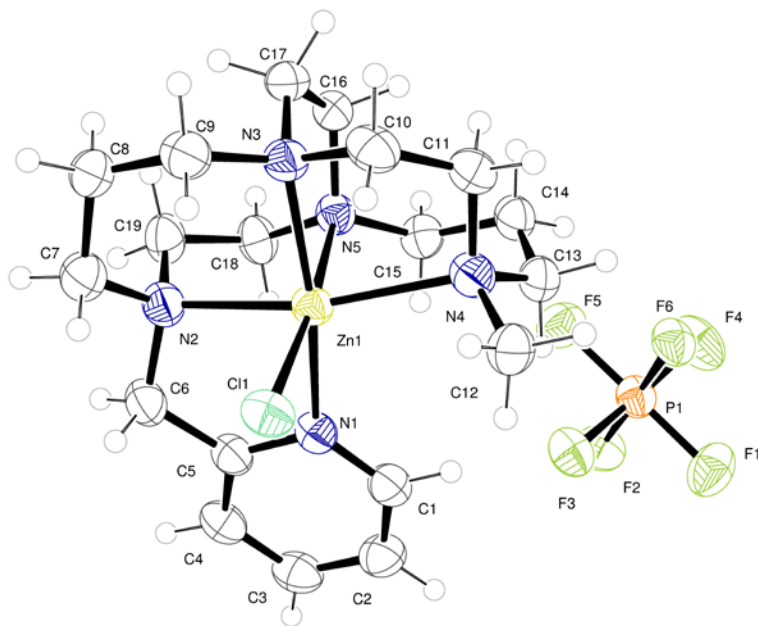


Figure 4. ORTEP representation of the asymmetric unit in **Zn-2**, [Zn(PyMeEBC)Cl]PF₆.

Atoms are drawn as 50 % probability ellipsoids. Atom colors: Zn yellow; Cl pale green; C gray; N blue; P orange; F yellow-green.



The ligand is again found to bind to the metal through each one of the five nitrogen atoms and the Cu²⁺ is formally five coordinate and no chloride is present in the crystal structure. The geometry about the metal may be described as a distorted trigonal bipyramid, with N2 and N4 occupying the axial positions and N1, N3, and N5 located in a trigonal plane. The coordination might also be described as distorted square-based pyramid (N3 as the peak), which highlights the vacant coordination site at the metal. (See **Figure 5**) The Addison Parameter [52] (τ) attempts to quantify the degree to which a 5-coordinate structure favors the ideal trigonal bipyramidal geometry ($\tau = 1$) or the ideal square pyramidal geometry ($\tau = 0$). For this structure, $t = 0.48$,

which indicates that the structure is nearly perfectly intermediate between these two ideals, and thus characterization as either extreme is inadequate.

The charge balancing in this structure is afforded by two PF_6^- anions, one of which forms a close approach to the metal, such that F12 is near to the vacant coordination site at the copper ion and the $\text{Cu1}\cdots\text{F12}$ distance is 3.104(3) Å. This is rather longer than the sum of the van der Waals radii [53] of these two ions (2.87 Å) and it is rather longer than the shortest such interactions present in similar systems reported in the Cambridge Structural Database. [54] For a copper ion, coordinated by four or five nitrogen atoms, $\text{Cu}\cdots\text{F}$ distances of around 2.7 Å are commonly observed and some much shorter examples are known *eg* refcode MINKAV has a $\text{Cu}\cdots\text{F}$ distance of 2.472 Å. It may be the case that this genuinely represents a weak interaction between the Cu^{2+} ion and the fluorine, but the fluorine is not very polarizable which suggest otherwise. It seems more likely that this close approach facilitates $\text{C-H}\cdots\text{F}$ interactions between the ligand and PF_6^- anion *ie* between F12 and H6B, H13B & H15B and other similar interactions involving the fluorine atoms of this anion.

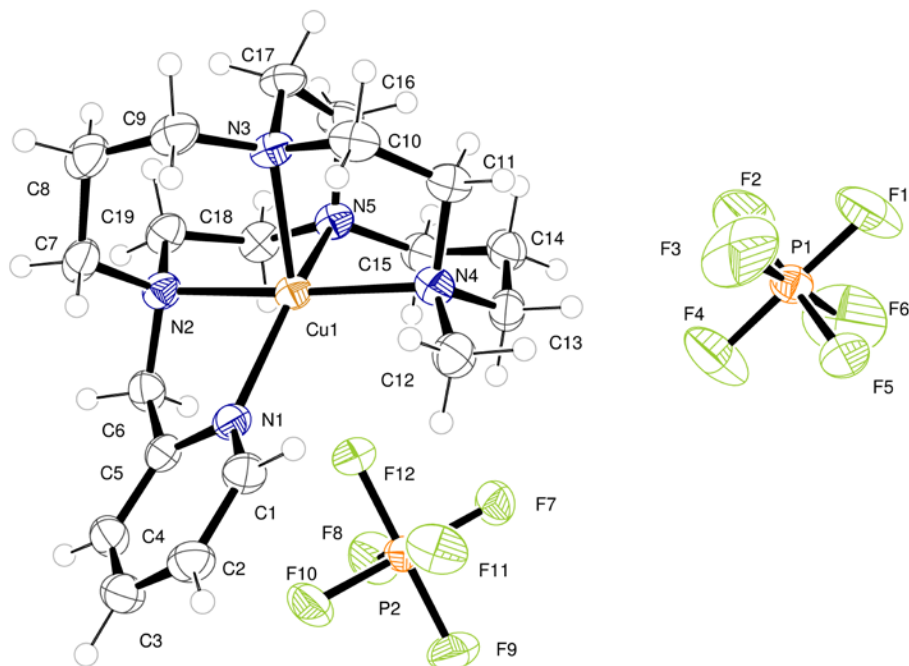


Figure 5. ORTEP representation of the asymmetric unit in $[\text{Cu}(\text{PyMeEBC})](\text{PF}_6)_2$. Atoms are drawn as 50 % probability ellipsoids. Atom colors: Cu bronze; C gray; N blue; P orange; F yellow-green.

A final comparison (**Table 1**) of all of the **PyMeEBC** structures is of interest, because all six divalent metal ions from Mn-Zn were coordinated and crystallized in very similar environments. A similar range of metal ions were crystallized in the parent ligand **Me₂EBC** [1] [55] [39] [51] [56] and a similar table, although less complete, has appeared previously. [56] In this comparison, the size of the metal ion is correlated to the $\text{N}_{\text{ax}}-\text{M}-\text{N}_{\text{ax}}$ and $\text{N}_{\text{eq}}-\text{M}-\text{N}_{\text{eq}}$ bond angles and generally shows a steady increase in these bond angles as the metal's ionic radius decreases and the bridged macrocycle is better able to engulf the metal ion with less distortion of the expected bond angles. Interestingly, for the larger ions Mn^{2+} and Fe^{2+} , the pyridine pendant arm of **PyMeEBC** allows coordination with much less distortion (6-7 degrees larger $\text{N}_{\text{ax}}-\text{M}-$

N_{ax} bond angles) than in their complexes with **Me₂EBC**. However this pendent arm effect is not present in the smaller metal ions, or at least more difficult to discern, as the identity of the non-macrocyclic ligands are not as directly comparable in some cases.

Table 1. Comparison of N—M—N bond angles for first row divalent metal ions with **Me₂EBC** and **PyMeEBC** from crystal structures. Except where noted, all complexes are high spin 6-coordinate $M(\text{Me}_2\text{EBC})\text{Cl}_2$ and $M(\text{PyMeEBC})\text{Cl}^+$, respectively.

		Me₂EBC		Ref	PyMeEBC	
Metal Ion	H.S. 6-coord. Ionic Radius	$N_{ax}\text{—}M\text{—}N_{ax}$	$N_{eq}\text{—}M\text{—}N_{eq}$		$N_{ax}\text{—}M\text{—}N_{ax}$	$N_{eq}\text{—}M\text{—}N_{eq}$
Mn²⁺	97	158.0(2)	75.6(2)	[1]	164.74(9)	78.40(10)
Fe²⁺	92	161.88(5)	78.36(5)	[1]	168.27(8)	80.82(8)
Co²⁺	89	172.4(2)	81.11(13)	[51]	172.34(12)	82.88(13)
Zn²⁺	88	[¶] 171.89(12)	[¶] 83.90(11)	[55]	168.66(avg)	81.84(avg)
Ni²⁺	83	[§] 175.39(5)	[§] 86.16(5)	[56]	173.56(avg)	84.85(avg)
Ni²⁺	83	[*] 174.56(10)	[*] 85.07(9)	[56]	---	---
Cu²⁺	[‡] 79	[‡] 175.16(13)	[‡] 85.30(12)	[39]	[‡] 175.66(13)	[‡] 85.24(12)
[¶] Zn(Me₂EBC)(OAc)(OH ₂) ⁺ [§] Ni(Me₂EBC)(OH ₂) ²⁺ [*] Ni(Me₂EBC)(acac) ⁺ [‡] Ionic radius and bond angles are for 5-coord complexes						

Crystallographic details for the seven new crystals structures in this work, along with selected bond lengths and angles, are presented in **Tables 2-3**.

Table 2. Crystallographic data. **L = PyMeEBC**

	[MnLCl]PF ₆ sja7_14 DGJ010B	[FeLCl]PF ₆ sja3_14 DGJ011	[CoLCl]PF ₆ sja4_14 DGJ012	[NiLCl]PF ₆ sja5_14 DGJ013	[CuL](PF ₆) ₂ sja2_14 DGJ014	[ZnLCl]PF ₆ sja1_14b DGJ015 form 1	[ZnLCl]PF ₆ sja1_14c DGJ015 form 2
Chemical Formula	[Mn(C ₁₉ H ₃₃ N ₅)Cl]PF ₆	[Fe(C ₁₉ H ₃₃ N ₅)Cl]PF ₆	[Co(C ₁₉ H ₃₃ N ₅)Cl]PF ₆	[Ni(C ₁₉ H ₃₃ N ₅)Cl]PF ₆	[Cu(C ₁₉ H ₃₃ N ₅)](PF ₆) ₂	[Zn(C ₁₉ H ₃₃ N ₅)Cl]PF ₆	[Zn(C ₁₉ H ₃₃ N ₅)Cl]PF ₆
a = ...(esd) Å	18.5536(10)	18.5989(9)	18.6711(13)	22.758(2)	10.5546(6)	22.794(3)	8.1050(6)
b = ...(esd) Å	8.6768(4)	8.6434(6)	8.6259(10)	13.730(2)	13.2043(11)	13.7535(9)	22.7534(14)
c = ...(esd) Å	14.9938(6)	14.8745(7)	14.8088(10)	15.0185(16)	18.6149(10)	15.1489(15)	12.5612(10)
α = ...(esd) degrees	90	90	90	90	90	90	90
β = ...(esd) degrees	90	90	90	93.047(8)	98.149(5)	93.512(9)	97.594(6)
γ = ...(esd) degrees	90	90	90	90	90	90	90
V = ... Å ³	2413.8(2)	2391.2(2)	2385.0(4)	4686.0(10)	2568.1(3)	4740.3(8)	2296.2(3)
Z =	4	4	4	8	4	8	4
Formula Weight	566.86	567.77	570.85	570.62	684.98	577.29	577.29
Space Group	P c a 2 ₁	P c a 2 ₁	P c a 2 ₁	P 2 ₁ /c	P 2 ₁ /c	P 2 ₁ /c	P 2 ₁ /c
T = ... °C	150(2)	150(2)	150(2)	150(2)	150(2)	150(2)	150(2)
λ = ... Å	0.71073	0.71073	0.71073	0.71073	0.71073	0.71073	0.71073
D ^{calcd} = ... g cm ⁻³	1.560	1.577	1.590	1.618	1.772	1.618	1.670
μ = ... mm ⁻¹	0.788	0.874	0.963	1.076	1.083	1.282	1.323
R1(F _o ²) =	0.0337	0.0263	0.0329	0.0452	0.0476	0.0504	0.0553
wR2(F _o ²) =	0.0848	0.0551	0.0637	0.1062	0.1265	0.1185	0.1451
R1 = Σ F _o - F _c / Σ F _o wR2 = {Σ [w(F _o ² - F _c ²) ²] / Σ [w(F _o ²) ²]} ^{1/2}							

Table 3. Selected Bond Lengths [Å] and angles [°].			
[Mn(PyMeEBC)Cl]PF₆		N(3)-Ni(1)-N(5)	84.75(11)
Mn(1)-N(1)	2.256(2)	N(3)-Ni(1)-N(1)	172.93(12)
Mn(1)-N(3)	2.257(3)	N(5)-Ni(1)-N(1)	93.39(12)
Mn(1)-N(4)	2.305(3)	N(3)-Ni(1)-N(2)	91.87(12)
Mn(1)-N(2)	2.299(3)	N(5)-Ni(1)-N(2)	84.38(12)
Mn(1)-N(5)	2.307(3)	N(1)-Ni(1)-N(2)	81.15(12)
Mn(1)-Cl(1)	2.4330(9)	N(3)-Ni(1)-N(4)	84.48(12)
N(1)-Mn(1)-N(3)	163.43(11)	N(5)-Ni(1)-N(4)	90.28(12)
N(1)-Mn(1)-N(2)	76.79(9)	N(1)-Ni(1)-N(4)	102.37(12)
N(3)-Mn(1)-N(2)	88.99(10)	N(2)-Ni(1)-N(4)	173.80(11)
N(1)-Mn(1)-N(4)	111.45(9)	N(3)-Ni(1)-Cl(1)	94.18(8)
N(3)-Mn(1)-N(4)	80.63(10)	N(5)-Ni(1)-Cl(1)	174.34(9)
N(2)-Mn(1)-N(4)	164.74(9)	N(1)-Ni(1)-Cl(1)	87.00(8)
N(1)-Mn(1)-N(5)	90.39(10)	N(2)-Ni(1)-Cl(1)	90.10(9)
N(3)-Mn(1)-N(5)	78.40(10)	N(4)-Ni(1)-Cl(1)	95.16(8)
N(2)-Mn(1)-N(5)	78.91(9)	N(13)-Ni(2)-N(15)	84.95(11)
N(4)-Mn(1)-N(5)	88.01(9)	N(13)-Ni(2)-N(12)	93.68(14)
N(1)-Mn(1)-Cl(1)	89.44(7)	N(15)-Ni(2)-N(12)	84.49(12)
N(3)-Mn(1)-Cl(1)	99.53(7)	N(13)-Ni(2)-N(11)	174.96(13)
N(2)-Mn(1)-Cl(1)	91.53(7)	N(15)-Ni(2)-N(11)	93.49(11)
N(4)-Mn(1)-Cl(1)	101.15(7)	N(12)-Ni(2)-N(11)	81.39(14)
N(5)-Mn(1)-Cl(1)	170.22(7)	N(13)-Ni(2)-N(14)	82.95(12)
[Fe(PyMeEBC)Cl]PF₆		N(15)-Ni(2)-N(14)	89.46(11)
Fe(1)-N(3)	2.204(2)	N(12)-Ni(2)-N(14)	173.32(11)
Fe(1)-N(1)	2.215(2)	N(11)-Ni(2)-N(14)	101.85(12)
Fe(1)-N(5)	2.232(2)	N(13)-Ni(2)-Cl(2)	94.79(8)
Fe(1)-N(2)	2.246(2)	N(15)-Ni(2)-Cl(2)	176.45(8)
Fe(1)-N(4)	2.285(2)	N(12)-Ni(2)-Cl(2)	91.99(9)
Fe(1)-Cl(1)	2.3805(7)	N(11)-Ni(2)-Cl(2)	86.47(8)
N(3)-Fe(1)-N(1)	167.98(9)	N(14)-Ni(2)-Cl(2)	94.02(8)
N(3)-Fe(1)-N(5)	80.82(8)	[Zn(PyMeEBC)Cl]PF₆ form 1	
N(1)-Fe(1)-N(5)	90.89(8)	Zn(1)-N(3)	2.157(4)
N(3)-Fe(1)-N(2)	92.17(9)	Zn(1)-N(1)	2.182(4)
N(1)-Fe(1)-N(2)	77.78(8)	Zn(1)-N(4)	2.221(4)
N(5)-Fe(1)-N(2)	80.29(8)	Zn(1)-N(5)	2.222(4)
N(3)-Fe(1)-N(4)	80.31(9)	Zn(1)-N(2)	2.225(4)
N(1)-Fe(1)-N(4)	108.49(8)	Zn(1)-Cl(1)	2.4123(14)
N(5)-Fe(1)-N(4)	89.58(8)	Zn(2)-N(13)	2.146(4)
N(2)-Fe(1)-N(4)	168.27(8)	Zn(2)-N(11)	2.196(4)
N(3)-Fe(1)-Cl(1)	98.15(6)	Zn(2)-N(12)	2.210(4)
N(1)-Fe(1)-Cl(1)	88.72(6)	Zn(2)-N(15)	2.222(3)
N(5)-Fe(1)-Cl(1)	171.26(6)	Zn(2)-N(14)	2.229(4)
N(2)-Fe(1)-Cl(1)	91.10(6)	Zn(2)-Cl(2)	2.3818(12)
N(4)-Fe(1)-Cl(1)	98.83(6)	N(3)-Zn(1)-N(1)	168.60(15)
[Co(PyMeEBC)Cl]PF₆		N(3)-Zn(1)-N(4)	83.94(15)
Co(1)-N(3)	2.157(3)	N(1)-Zn(1)-N(4)	105.60(15)
Co(1)-N(5)	2.175(3)	N(3)-Zn(1)-N(5)	81.59(14)
Co(1)-N(1)	2.177(3)	N(1)-Zn(1)-N(5)	92.25(15)
Co(1)-N(2)	2.206(3)	N(4)-Zn(1)-N(5)	88.59(15)
Co(1)-N(4)	2.263(3)	N(3)-Zn(1)-N(2)	90.17(15)
Co(1)-Cl(1)	2.3989(12)	N(1)-Zn(1)-N(2)	79.40(14)
N(3)-Co(1)-N(5)	82.88(13)	N(4)-Zn(1)-N(2)	169.23(15)
N(3)-Co(1)-N(1)	171.69(14)	N(5)-Zn(1)-N(2)	81.62(15)
N(5)-Co(1)-N(1)	92.69(13)	N(3)-Zn(1)-Cl(1)	96.48(11)
N(3)-Co(1)-N(2)	93.59(13)	N(1)-Zn(1)-Cl(1)	88.61(11)
N(5)-Co(1)-N(2)	81.90(12)	N(4)-Zn(1)-Cl(1)	97.19(12)
N(1)-Co(1)-N(2)	78.78(12)	N(5)-Zn(1)-Cl(1)	173.70(11)
N(3)-Co(1)-N(4)	81.55(13)	N(2)-Zn(1)-Cl(1)	92.42(12)
N(5)-Co(1)-N(4)	91.59(12)	N(13)-Zn(2)-N(11)	170.23(15)
N(1)-Co(1)-N(4)	105.68(12)	N(13)-Zn(2)-N(12)	92.06(16)
N(2)-Co(1)-N(4)	172.34(12)	N(11)-Zn(2)-N(12)	79.30(15)
N(3)-Co(1)-Cl(1)	95.69(10)	N(13)-Zn(2)-N(15)	82.17(14)
N(5)-Co(1)-Cl(1)	171.36(9)	N(11)-Zn(2)-N(15)	91.96(14)
N(1)-Co(1)-Cl(1)	87.64(9)	N(12)-Zn(2)-N(15)	81.55(14)
N(2)-Co(1)-Cl(1)	89.71(9)	N(13)-Zn(2)-N(14)	83.38(14)
N(4)-Co(1)-Cl(1)	96.63(9)	N(11)-Zn(2)-N(14)	104.37(14)
[Cu(PyMeEBC)](PF₆)₂		N(12)-Zn(2)-N(14)	169.59(14)
Cu(1)-N(2)	2.046(3)	N(15)-Zn(2)-N(14)	88.55(13)

Cu(1)-N(4)	2.079(3)	N(13)-Zn(2)-Cl(2)	96.97(10)
Cu(1)-N(1)	2.125(3)	N(11)-Zn(2)-Cl(2)	88.12(10)
Cu(1)-N(5)	2.135(3)	N(12)-Zn(2)-Cl(2)	93.06(11)
Cu(1)-N(3)	2.136(3)	N(15)-Zn(2)-Cl(2)	174.49(10)
N(2)-Cu(1)-N(4)	175.66(13)	N(14)-Zn(2)-Cl(2)	96.77(10)
N(2)-Cu(1)-N(1)	79.27(12)	[Zn(PyMeEBC)Cl]PF ₆ form 2	
N(4)-Cu(1)-N(1)	104.95(12)	Zn(1)-N(3)	2.163(3)
N(2)-Cu(1)-N(5)	84.54(13)	Zn(1)-N(4)	2.256(3)
N(4)-Cu(1)-N(5)	91.27(13)	Zn(1)-N(5)	2.249(3)
N(1)-Cu(1)-N(5)	146.87(12)	Zn(1)-N(2)	2.210(3)
N(2)-Cu(1)-N(3)	91.64(12)	Zn(1)-N(1)	2.183(3)
N(4)-Cu(1)-N(3)	86.85(12)	Zn(1)-Cl(1)	2.4043(10)
N(1)-Cu(1)-N(3)	123.66(12)	N(3)-Zn(1)-N(1)	167.98(12)
N(5)-Cu(1)-N(3)	85.24(12)	N(3)-Zn(1)-N(2)	89.81(11)
[Ni(PyMeEBC)Cl]PF ₆		N(1)-Zn(1)-N(2)	79.94(11)
Ni(1)-N(3)	2.101(3)	N(3)-Zn(1)-N(5)	81.76(11)
Ni(1)-N(5)	2.127(3)	N(1)-Zn(1)-N(5)	90.42(10)
Ni(1)-N(1)	2.129(3)	N(2)-Zn(1)-N(5)	81.26(11)
Ni(1)-N(2)	2.153(3)	N(3)-Zn(1)-N(4)	83.32(11)
Ni(1)-N(4)	2.200(3)	N(1)-Zn(1)-N(4)	105.49(11)
Ni(1)-Cl(1)	2.4310(9)	N(2)-Zn(1)-N(4)	167.17(11)
Ni(2)-N(13)	2.095(3)	N(5)-Zn(1)-N(4)	87.02(11)
Ni(2)-N(15)	2.122(3)	N(3)-Zn(1)-Cl(1)	97.38(8)
Ni(2)-N(12)	2.125(3)	N(1)-Zn(1)-Cl(1)	89.60(8)
Ni(2)-N(11)	2.135(3)	N(2)-Zn(1)-Cl(1)	93.77(8)
Ni(2)-N(14)	2.223(3)	N(5)-Zn(1)-Cl(1)	174.94(8)
Ni(2)-Cl(2)	2.3923(9)	N(4)-Zn(1)-Cl(1)	97.84(8)

Electronic Structure

Solid state magnetic moments were determined for all five paramagnetic **PyMeEBC** complexes. [Mn(**PyMeEBC**)Cl]PF₆ gave a magnetic moment of $\mu_{\text{eff}} = 5.47$, which is slightly lower than the expected value (5.65-6.10), [57] but clearly indicative of a high spin d^5 Mn²⁺ ion. The other paramagnetic complexes had magnetic moments within the expected ranges for high spin divalent metal ions: [Fe(**PyMeEBC**)Cl]PF₆ $\mu_{\text{eff}} = 5.28$, [Co(**PyMeEBC**)Cl]PF₆ $\mu_{\text{eff}} = 4.61$, [Ni(**PyMeEBC**)Cl]PF₆ $\mu_{\text{eff}} = 2.91$, and [Cu(**PyMeEBC**)]PF₆ $\mu_{\text{eff}} = 1.79$. This high spin behavior is similar to the divalent first row transition metal complexes of **Me₂EBC**. [1] [39] [51] [56] Apparently, addition of the pyridine donor, in place of a typically chloro ligand or oxygen donor in the **Me₂EBC** complexes, does not cause a change from high spin to low spin, even though pyridine is typically a stronger field ligand.

Table 4 contains absorbances and extinction coefficients for the six complexes of **PyMeEBC**. The electronic spectra of the zinc complex, with only ligand-based absorbances likely, was

obtained to help differentiate these absorbances from the metal ion based absorbances of the other complexes. $\text{Zn}(\text{PyMeEBC})\text{Cl}^+$ had two peaks at 317 nm ($\epsilon = 220 \text{ M}^{-1}\text{cm}^{-1}$) and 264 nm ($\epsilon = 4120 \text{ M}^{-1}\text{cm}^{-1}$). The high spin Mn^{2+} and Fe^{2+} complexes showed no d-d bands, which is typical of for ligands of this type, and the same behavior is observed for $\text{Mn}(\text{Me}_2\text{EBC})\text{Cl}_2$ and $\text{Fe}(\text{Me}_2\text{EBC})\text{Cl}_2$. [1] $\text{Fe}(\text{Me}_2\text{EBC})\text{Cl}_2$ has a weak shoulder at 350 nm ($\epsilon = 260 \text{ M}^{-1}\text{cm}^{-1}$) that is not present in the manganese complex. Likewise, there is an additional absorbance for $\text{Fe}(\text{PyMeEBC})\text{Cl}^+$ at 403 nm ($\epsilon = 225 \text{ M}^{-1}\text{cm}^{-1}$). This band is likely associated with the chloro ligand as the presence of the similar band in $\text{Fe}(\text{Me}_2\text{EBC})\text{Cl}_2$ is not dependent on the pyridine.

The electronic spectrum of the cobalt complex is similar to those of other high spin octahedral cobalt(II) complexes, having a single major absorption typically between about 500 and 600 nm. This band is due to the ${}^4\text{T}_{1g}(\text{P}) \rightarrow {}^4\text{T}_{1g}(\text{D})$ transition. [58] The $\text{Co}(\text{PyMeEBC})\text{Cl}^+$ absorbance is at 499 nm ($\epsilon = 34 \text{ M}^{-1}\text{cm}^{-1}$), which is similar to the $\text{Co}(\text{Me}_2\text{EBC})\text{Cl}_2$ complex which absorbs at 540 nm ($\epsilon = 24 \text{ M}^{-1}\text{cm}^{-1}$). [51]

$\text{Ni}(\text{PyMeEBC})\text{Cl}^+$ exhibits a classic octahedral Ni^{2+} spectrum with three major absorbances between 300-100 nm in acetonitrile. [58] This spectrum allows us to determine the ligand field strength, which is taken as the energy of the lowest energy absorption band. [59] In this case, the absorption at 891 nm ($\epsilon = 13 \text{ M}^{-1}\text{cm}^{-1}$) converts to $\Delta_o = 11,223 \text{ cm}^{-1}$. In comparison, $\text{Ni}(\text{Me}_2\text{EBC})\text{Cl}_2$ gave $\Delta_o = 10,215 \text{ cm}^{-1}$ from a similar calculation. Clearly, the pendant pyridine donor increases the ligand field strength, as might be expected for replacement of one chloro ligand by a pyridine. Yet, as shown by the magnetic moment data above, all of the complexes remain high spin.

The Cu(PyMeEBC)²⁺ complex exhibits the expected d⁹ Cu²⁺ d-d band at 639 nm ($\epsilon = 101 \text{ M}^{-1}\text{cm}^{-1}$). This compares to the analogous absorption at 671 nm ($\epsilon = 100 \text{ M}^{-1}\text{cm}^{-1}$) for Cu(Me₂EBC)Cl⁺. [39] Interestingly, Cu(PyMeEBC)²⁺ has an additional broad peak stretching from 830-1200 nm with its maximum at 1042 nm ($\epsilon = 42 \text{ M}^{-1}\text{cm}^{-1}$) that is not normally observed for this ion. Cu²⁺ complexes typically have only a single absorbance in the visible region representing up to three different unresolved transitions. [58] However, trigonal and tetragonal distortions can lead to one higher intensity band in the visible range and one lower intensity band in the near infrared. [58] The exact nature of the distortion is difficult to assign based on the spectrum alone. Fortunately, the obtained X-ray crystal structure confirms a tetragonally distorted 5-coordinate structure for Cu(PyMeEBC)²⁺ that may give rise to its electronic spectrum.

Table 4. Electronic spectra of M(PyMeEBC) complexes in acetonitrile.

complex	ligand-based and charge transfer bands, nm ($\epsilon, \text{M}^{-1}\text{cm}^{-1}$)	d—d bands, nm ($\epsilon, \text{M}^{-1}\text{cm}^{-1}$)
Zn(PyMeEBC)Cl ⁺	317(220), 264(4120)	-----
Mn(PyMeEBC)Cl ⁺	322(266), 263(4460)	-----
Fe(PyMeEBC)Cl ⁺	403(225), 317(230), 263(4550)	-----
Co(PyMeEBC)Cl ⁺	323(650), 259(8150)	499(34)
Ni(PyMeEBC)Cl ⁺	310(177), 264(3730)	891(13), 551sh(19), 422sh(42)
Cu(PyMeEBC) ²⁺	286(5240), 264(7430)	639(101), 1042(42)

Electrochemical Studies

Table 5. Redox potentials (vs. SHE) with peak separations for PyMeEBC and Me₂EBC complexes. (If no reference is listed, the data is from this work.)

complex	redox process	potential (V)	peak separation (mV)	ref.
Mn(PyMeEBC)Cl ⁺	Mn ⁺ /Mn ²⁺	E _{1/2} = -0.526	246	
	Mn ²⁺ /Mn ³⁺	E _{1/2} = +0.812	74	
	Mn ³⁺ /Mn ⁴⁺	E _{1/2} = +1.744	286	
Mn(Me ₂ EBC)Cl ₂	Mn ²⁺ /Mn ³⁺	E _{1/2} = +0.585	61	[1]
	Mn ³⁺ /Mn ⁴⁺	E _{1/2} = +1.343	65	[1]
Fe(PyMeEBC)Cl ⁺	Fe ⁺ /Fe ²⁺	E _{1/2} = -1.969	126	
	Fe ²⁺ /Fe ³⁺	E _{1/2} = +0.563	82	
Fe(Me ₂ EBC)Cl ₂	Fe ²⁺ /Fe ³⁺	E _{1/2} = +0.110	63	[1]
Co(PyMeEBC)Cl ⁺	Co ⁺ /Co ²⁺	E _{1/2} = -1.386	143	
	Co ⁺ →Co ²⁺	E _{ox} = -1.200	---	
	Co ²⁺ /Co ³⁺	E _{1/2} = +0.657	154	
Co(Me ₂ EBC)Cl ₂	Co ²⁺ →Co ⁺	E _{red} = -2.198	---	[51]
	Co ²⁺ /Co ³⁺	E _{1/2} = +0.173	103	[51]
Ni(PyMeEBC)Cl ⁺	Ni ²⁺ →Ni ⁺	E _{red} = -1.026	---	
	Ni ²⁺ →Ni ³⁺	E _{ox} = +1.290	---	
Ni(Me ₂ EBC)Cl ₂	Ni ²⁺ →Ni ⁺	E _{red} = -1.894	---	[56]
	Ni ²⁺ /Ni ³⁺	E _{1/2} = +0.991	154	[56]
Cu(PyMeEBC) ²⁺	Cu ⁺ /Cu ²⁺	E _{1/2} = -0.402	80	
Cu(Me ₂ EBC)Cl ⁺	Cu ²⁺ →Cu ⁺	E _{red} = -0.544	---	[60]
	Cu ²⁺ →Cu ³⁺	E _{ox} = +1.530	---	[60]

In selecting **PyMeEBC** as a target for development of oxidation catalysts based on **Me₂EBC**, we expected addition of the pyridine donor to lead to changes in the electrochemistry of the resulting complexes. **Table 5** shows the potential and peak separation for the Mn-Cu complexes of both of these ligands. **Figure 6** shows the cyclic voltammograms of all **PyMeEBC** complexes. Three main trends can be observed in examining this data. The two manganese complexes, Mn(PyMeEBC)Cl⁺ and Mn(Me₂EBC)Cl₂, will be used to illustrate the trends, which generally hold for all five metals (Mn-Cu) examined.

(1) Oxidation is significantly more positive for the **PyMeEBC** complexes. The $\text{Mn}^{2+}/\text{Mn}^{3+}$ redox couple is at +0.812 V for the **PyMeEBC** complex, while this value is +0.585 V for the **Me₂EBC** complex. Similarly, the $\text{Mn}^{3+}/\text{Mn}^{4+}$ couples are at +1.744 V and +1.343 V for **PyMeEBC** and **Me₂EBC**, respectively. A simple explanation for this behavior is the replacement of a negatively charged chloro ligand with a neutral pyridine donor in **PyMeEBC**. The two negatively charged chloro ligands in the **Me₂EBC** complexes clearly favor oxidation compared to the single chloro and pyridine donor in **PyMeEBC**. Access to stable species at higher oxidation potentials may allow oxidation processes with more difficult-to-oxidize substrates, if this property is present in catalytically active species of the **PyMeEBC** complexes.

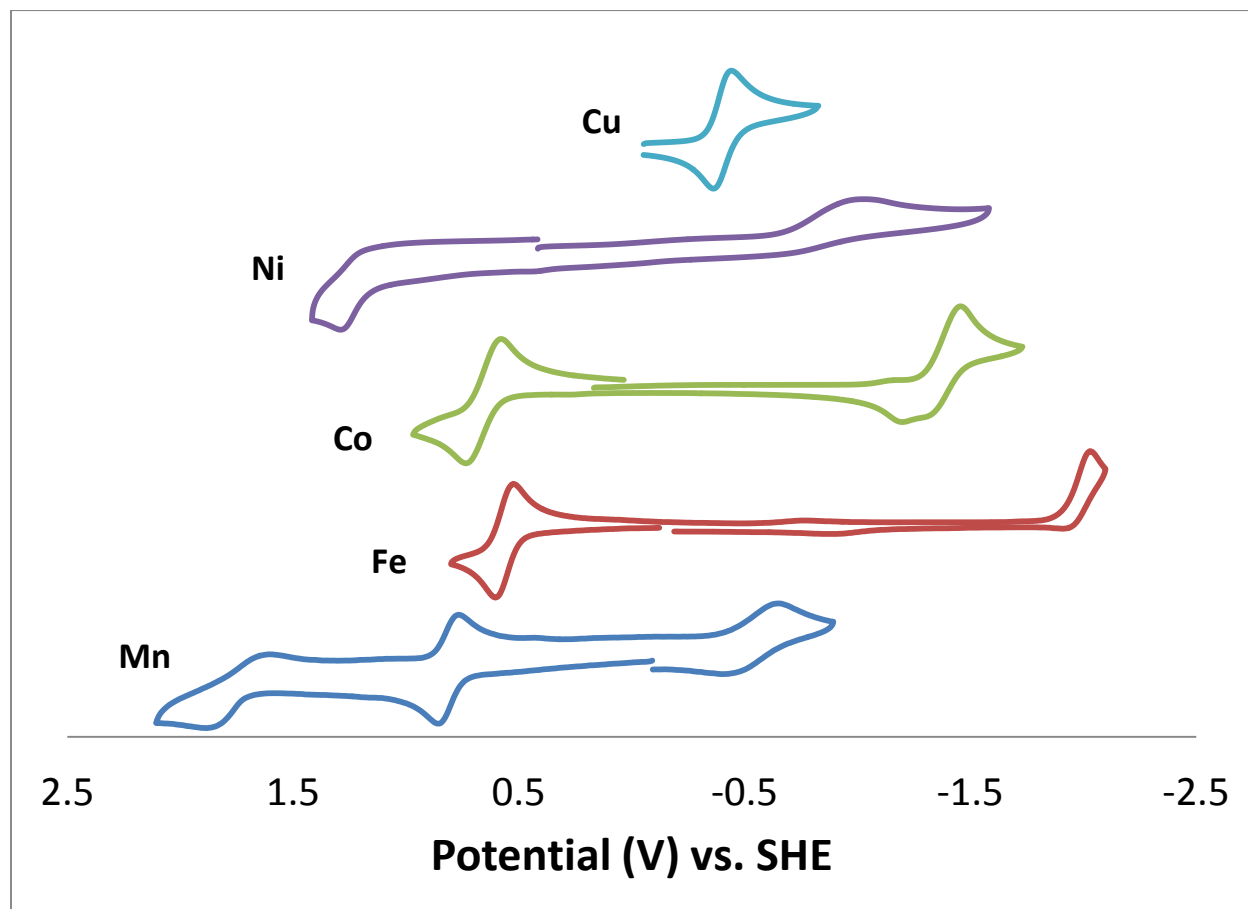
(2) Reduction is significantly easier for the **PyMeEBC** complexes. One less negatively charged chloro ligand allows reversible reduction to occur in acetonitrile for the Mn complex of **PyMeEBC** (at -0.526 V), whereas this reduction is not observed at all for the Mn complex of **Me₂EBC**.

(3) A general trend towards reversible access to a larger range of oxidation states is observed in most cases for the **PyMeEBC** ligand (see **Figure 6**). Reversible access to $\text{Mn}^+/\text{Mn}^{2+}/\text{Mn}^{3+}/\text{Mn}^{4+}$, $\text{Fe}^+/\text{Fe}^{2+}/\text{Fe}^{3+}$, $\text{Co}^+/\text{Co}^{2+}/\text{Co}^{3+}$, and $\text{Cu}^+/\text{Cu}^{2+}$ are observed for the **PyMeEBC** complexes, whereas reversible access for **Me₂EBC** complexes is restricted to $\text{Mn}^{2+}/\text{Mn}^{3+}/\text{Mn}^{4+}$, $\text{Fe}^{2+}/\text{Fe}^{3+}$, $\text{Co}^{2+}/\text{Co}^{3+}$, and only Cu^{2+} . Catalytic processes would require reversible access to multiple oxidation states, although the utility for oxidation catalysis of reversibly accessing the M^+ oxidation states in the **PyMeEBC** complexes is not obvious.

Interestingly, neither oxidation to Ni^{3+} nor reduction to Ni^+ is reversible for $\text{Ni}(\text{PyMeEBC})\text{Cl}^+$, even though the $\text{Ni}^{2+}/\text{Ni}^{3+}$ redox couple is reversible for $\text{Ni}(\text{Me}_2\text{EBC})\text{Cl}_2$. Perhaps two chloro ligands are required to stabilize the Ni^{3+} ion, when only one is present in $\text{Ni}(\text{PyMeEBC})\text{Cl}^+$.

Similarly, the lack of even one chloro ligand in $\text{Cu}(\text{PyMeEBC})^{2+}$ eliminates the oxidation to Cu^{3+} altogether, even though a non-reversible oxidation to Cu^{3+} is observed (+1.530 V) for $\text{Cu}(\text{Me}_2\text{EBC})\text{Cl}^+$. However, the $\text{Cu}^+/\text{Cu}^{2+}$ redox process is reversible for $\text{Cu}(\text{PyMeEBC})^{2+}$, though non-reversible for $\text{Cu}(\text{Me}_2\text{EBC})\text{Cl}^+$. In the latter complex, loss of the chloro ligand upon reduction to Cu^+ is reasonable and is supported by a related 4-coordinate copper(I) complex crystal structure. [61] Loss of the fifth (pyridine) donor is not likely for $\text{Cu}(\text{PyMeEBC})^{2+}$ because the pyridine donor is neutral and, probably more important, because it is covalently bound to the rest of the ligand.

Figure 6. Cyclic voltammograms for $\text{Cu}(\text{PyMeEBC})^{2+}$, $\text{Ni}(\text{PyMeEBC})\text{Cl}^+$, $\text{Co}(\text{PyMeEBC})\text{Cl}^+$, $\text{Fe}(\text{PyMeEBC})\text{Cl}^+$, $\text{Mn}(\text{PyMeEBC})\text{Cl}^+$.



Catalytic Oxidation Screening

Screening for the oxidation reactivity of the biologically relevant Mn, Fe, and Cu complexes in catalytic processes may not only help understand the behaviors of related metalloenzymes, but guide the exploration of these complexes' potential applications. In the electrochemical studies above, it has been observed that **PyMeEBC** ligated metal ions demonstrate reversible redox behaviors, which provides the basis to explore their catalytic activity in oxidations.

Hydrogen Abstraction (HAT)

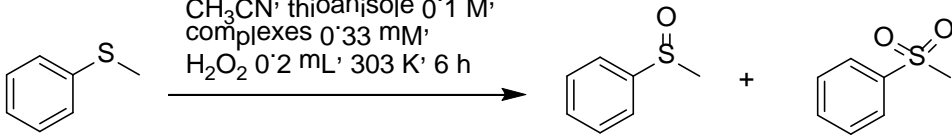
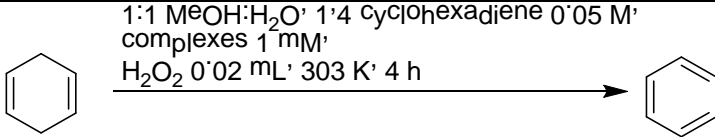
The catalytic oxidation properties of the Mn^{2+} , Fe^{2+} and Cu^{2+} complexes were first investigated in hydrogen abstraction (**Table 10**), which is the most fundamental process in redox chemistry. [62] Using 1,4-cyclohexadiene as substrate with H_2O_2 oxidant, after reaction at 303 k for 4 h in acetonitrile, the manganese(II) complex of **PyMeEBC** produces 51.2% yield of benzene with 88.0% conversion, while the corresponding iron(II) complex yields only 33.3% of benzene with 55.3% conversion. Since these two complexes are isostructural (*vide supra*) these functional differences clearly have electronic/electrochemical rather than structural origins. The higher oxidation potential of the $\text{Mn}^{2+/3+}$ couple compared to the $\text{Fe}^{2+/3+}$ couple, and access to Mn^{4+} , while Fe^{4+} is not available, as discussed in the electrochemistry section, likely explains the more efficient hydrogen atom abstraction.

Compared with the high conversion, the relatively low yield of benzene with the manganese(II) **PyMeEBC** complex is possibly related to its oxygen transfer activity which leads to formation of epoxide (*vide infra*), but the products were not identified in GC analysis. In comparison, the manganese(II) complex with the **Me₂EBC** ligand is much more active, and gives 71.4% yield of benzene with 86.2% conversion. A multitude of other synthetic manganese complexes have shown excellent catalytic hydrogen abstraction ability, so this is not unique or unexpected. However, it

is reassuring that addition of a fifth donor atom to the cross-bridged cyclam chelate has not eliminated this reactivity for Mn(PyMeEBC) and future studies will aim at elucidating the mechanism of hydrogen atom abstraction by Mn(PyMeEBC).

The copper(II) complex of PyMeEBC is very sluggish as a catalyst for hydrogen abstraction—the yield of benzene is close to its natural content in commercial 1,4-cyclohexadiene (~3%). The lack of reactivity of the Cu complex is most logically explained not by its structure, which is in fact different from the isostructural Fe and Mn complexes, yet does retain the entire 5-coordinate PyMeEBC ligand, but rather its electrochemistry, which lacks any oxidation states above Cu²⁺ and suggests that this is just not reactive enough to result in substrate oxidation.

Table 6. Oxidation catalysis screening results for manganese(II), iron(II), and copper(II) complexes of PyMeEBC, in comparison to Mn(Me₂EBC)Cl₂.

			
Complex	Conversion %	Yield % Sulfoxide	Yield % Sulfone
Mn(Me ₂ EBC)Cl ₂	99.8	44.3	46.5
[Mn(PyMeEBC)Cl]Cl	75.3	53.9	14.1
[Fe(PyMeEBC)Cl]PF ₆	47.2	30.1	12.5
[Cu(PyMeEBC)](PF ₆) ₂	11.7	9.2	0.71
			
Complex	Conversion %	Yield % Benzene	
Mn(Me ₂ EBC)Cl ₂	86.2	71.4	
[Mn(PyMeEBC)Cl]Cl	88.0	51.2	
[Fe(PyMeEBC)Cl]PF ₆	55.3	33.3	
[Cu(PyMeEBC)](PF ₆) ₂	23.2	3.7	

Oxygen Atom Transfer (OAT)

For oxygen atom transfer screening, thioanisole was selected as substrate and acetonitrile was employed as solvent with H_2O_2 oxidant. After reaction at 303 K for 6 h, the manganese(II) **PyMeEBC** complex gives 53.9% yield of sulfoxide with 14.1% of sulfone, while the conversion is 75.3%. The iron(II) complex gives 30.1% of sulfoxide and 12.5% of sulfone with 47.2% conversion. Similar to the hydrogen abstraction experiment, the copper(II) complex is inactive for sulfide oxidation, with results comparable with those from the control experiment without catalyst.

Again the Mn(**Me₂EBC**) is more active in sulfide oxidation, yielding 44.3% of sulfoxide and 46.5% of sulfone with almost complete conversion of sulfide. In comparison, Mn(**PyMeEBC**) only produces 14.1% sulfone with most of its product (53.9%) the sulfoxide, and only 75.3% conversion. It appears that addition of the 2-pyridylmethyl pendant arm has lowered the overall reactivity (less conversion and less sulfone) but improved the selectivity for the sulfoxide product. As shown in **Table 9**, the redox potential of the $\text{Mn}^{3+}/\text{Mn}^{4+}$ couple for Mn(**Me₂EBC**)Cl₂ is substantially lower than that for Mn(**PyMeEBC**)Cl⁺ (+1.343 vs +1.744 V). Also, the peak separation shows that Mn(**Me₂EBC**)Cl₂ is electrochemically reversible while the reversibility is not so good for Mn(**PyMeEBC**)Cl⁺. Clearly, oxidizing Mn(**PyMeEBC**)Cl⁺ to the corresponding manganese(IV) complex is not so easy as Mn(**Me₂EBC**)Cl₂ where the manganese(IV) complex can be obtained in large scale, and this may explain its relatively poor efficiency in sulfide oxygenation in which the manganese(IV) species may play significant roles. [12]

In terms of utility, this selectivity for sulfoxide production may be advantageous. Organic sulfoxides are useful synthetically for the production of pharmaceuticals and other valuable chemical compounds. [63] [64] A number of synthetic manganese catalysts have been developed that can efficiently transform sulfides into sulfoxides and/or sulfones. [64] [65] [66] [67] [68] [69]

The closest literature analogs to Mn(**Me₂EBC**) and Mn(**PyMeEBC**) are probably the manganese complexes of 1,4,7-trimethyl-1,4,7-triazacyclononane (**TMTACN**), [67] [68] [69] which generally demonstrate a more efficient sulfide oxygenation activity. In this catalyst, a manganese(V) oxo intermediate was proposed to serve as the oxygenation species by concerted oxygen transfer or electron transfer mechanism, leading to sulfoxide and then sulfone products in two oxidation steps. The Mn-**TMTACN** catalysts were developed as bleach catalysts for the laundry industry and were actually introduced into consumer products. Yet, their lack of selectivity in oxidation reactivity contributed to their removal from those consumer products due to damaging cloth. [69] Although Mn(**PyMeEBC**) does not appear to be as highly efficient as some of these other catalysts based on the above initial screening data, we look forward to future studies aimed at fully understanding its oxidation mechanisms and attempting to optimize its sulfoxidation selectivity.

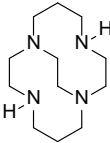
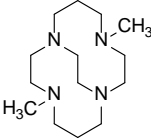
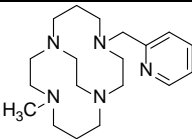
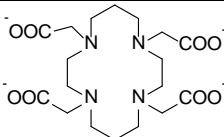
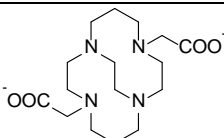
Although these catalytic oxidations are very preliminary, with further mechanistic elucidation the subject of future work, they have provided useful information regarding the potential applications of these metal complexes with the **PyMeEBC** ligand. Another potential application where selective, mild oxidation, in addition to the formation of sulfoxides rather than sulfones, is the laundry industry. Here, a good catalyst should be efficient enough to oxygenate the soil for its removal from clothes, but must be sluggish enough in hydrogen atom abstraction to avoid damage of cotton or other textiles. [16] [17] [18] [19] [20] The manganese(II) complex with **Me₂EBC** has demonstrated its ability to serve as a redox catalyst in detergent, but has not yet been embraced by the industry, perhaps because it is too reactive. [16] [17] [18] [19] [20] Here, the manganese(II) complex with **PyMeEBC** seems to be even more attractive as a detergent catalyst, because it has a comparable oxygenation efficiency as the Mn(**Me₂EBC**)²⁺ complex, while its hydrogen

abstraction power is desirably more sluggish. More detailed studies on this issue are still in progress to explore the potentially useful redox chemistry of **PyMeEBC** complexes.

Kinetic Stability

A particularly useful property of cross-bridged tetraazamacrocycle complexes due to their topological complexity and the rigidity caused by their small size, is their typically extreme stability under harsh conditions. [1] [2] [3] [4] As established by Busch [70] [1] and standardized by Weisman, [71] [72] [73] [74] probing the stability of new cross-bridged ligands is now routinely done using the copper(II) complex, which is often the first (or only) transition metal complex synthesized due to the interest in PET imaging applications of ^{64}Cu . Weisman has chosen 5 M HCl and various temperature points, such as 30 °C, 50 °C, and 90 °C as benchmarks for kinetic stability of new Cu cross-bridged complexes. Unfortunately, the proton-sponge nature of these ligands prevents aqueous titration in the presence of a metal ion to yield formation constants, as the ligand never gives up its last proton(s) and the complex is not formed. Instead, kinetic decomplexation studies in the presence of high acid concentration under pseudo first order conditions is used to give some measure of complex stability. Currently, only copper(II) complexes have undergone these studies and yielded published data for comparison.

Although $\text{Cu}(\text{Me}_2\text{EBC})\text{Cl}^+$ was the first cross-bridged complex to undergo this sort of experiment,[50] the 1 M HClO_4 and 40 °C conditions used make comparison to Weisman's database of compounds difficult. We have, therefore, resynthesized this complex and tested it, as well as $\text{Cu}(\text{PyMeEBC})^{2+}$, in order to determine the effects of adding the 2-pyridylmethyl pendant arm to the ethylene cross-bridged ligand. Results of the decomplexation studies are presented in **Table 7**, along with relevant literature data for comparison.

Table 7. Half-lives of selected copper(II) complexes in 5 M HCl				
Complex	50 °C	90 °C	reference	Ligand Structure
Cu(H₂EBC)	-----	11.8 min	[71]	
Cu(Me₂EBC)	7.3 d	79 min	this work	
Cu(PyMeEBC)	14.7 min	< 2 min	this work	
Cu(TETA)	3.2 hour	4.5 min	[71]	
Cu(CB-TE2A)	-----	154 hour	[71]	

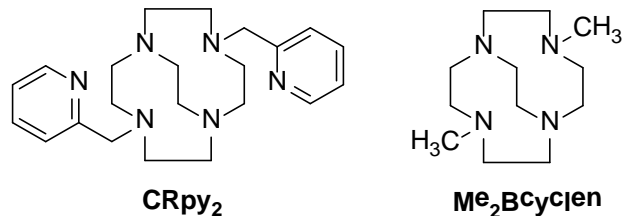
According to the teachings of coordination chemistry, [75] if we add additional chelate rings, a polydentate ligand typically forms more stable transition metal complexes, as long as the metal-ligand match in size, geometry, and electronics is not perturbed. For example, Weisman's bis-carboxylate pendant arm cross-bridged ligand **CB-TE2A** (Table 7), gains up to 4 orders of magnitude in stability versus the **H₂EBC** complex, as seen in Table 7. In contrast, the stability of the copper(II) complex decreases, from a 79 minute half-life for tetradentate **Me₂EBC** at 90 °C in 5 M HCl to less than 2 minutes for pentadentate **PyMeEBC**, even though an additional chelate ring involving the pyridine pendant arm has been added to the structure. A similar, and more

easily measurable, decrease in stability was observed at 50 °C, from 7.3 days, to 14.7 minutes, respectively.

This appears to be the first example of subtraction of stability upon addition of chelating groups to a cross-bridged tetraazamacrocyclic parent structure. Perhaps the strain noted for the 4-membered chelate rings involving the pyridine donors ($N(2)-Cu(1)-N(1) = 79.27(12)^\circ$) in the discussion of the X-ray crystal structures above reveals that the geometry match between metal and ligand is disrupted by the pyridine pendant arm, making dissociation easier. Weisman's **Cu(CB-TE2A)** can actually protonate one of the acetate pendant arms without dissociating either chelate arm—likely a key to its acid stability. Perhaps telling is that the chelate bond angle for the O-Cu-N chelate ring of the acetate pendant arm that does not protonate is a much less strained $84.03(7)^\circ$, according to a crystal structure of the monoprotonated complex. [71] Whatever the mechanism, addition of the pyridine pendant arm clearly destabilizes its copper(II) complex towards acid decomplexation when compared to other cross-bridged cyclam ligands, and even the unbridged ligand **TETA** is more stable towards decomplexation under the same conditions (**Table 7**).

Interestingly, the Cu^{2+} complex of a bis-(2-pyridylmethyl)-pendant armed cross-bridged cyclen (**CRpy₂**, **Figure 7**) ligand is in fact stabilized towards acid decomplexation compared to its dimethyl analog (**Me₂Bcyclen**). [36] In this case **CRpy₂** is lost at 25 °C in 3 M HClO₄ with an estimated half-life of 7 days, while the dimethyl ligand is lost from Cu^{2+} at 25 °C in 1 M HClO₄ with a half-life of 30 hours. [60] No crystal structure of the Cu-**CRpy₂** ligand was obtained, so strain arguments can't be used in this case. Why one pyridine pendant arm destabilizes a given copper complex, while two pyridine pendant arms stabilize another in a compelling problem.

Figure 7. Cross-bridged cyclen ligands discussed.



Even though its copper complex is destabilized toward strong acid decomplexation, the copper(II), iron(II), and manganese(II) complexes of **PyMeEBC** gave no visual signs of decomplexation during the oxidation catalysis screening reactions discussed above. Manganese and iron complexes typically give insoluble oxide precipitates under oxidizing conditions, such as the hydrogen peroxide conditions used in the oxidation reactions tested. No precipitates were observed during these reactions, qualitatively indicating sufficient stability under the conditions used. Additional stability experiments for these complexes will accompany the mechanistic experiments planned to fully understand their redox catalysis.

Conclusions

A new pyridylmethyl N-pendant arm cross-bridged cyclam ligand, **PyMeEBC**, has been synthesized with a key synthetic step using non-polar chloroform as the solvent to reduce the self-reactivity of picolyl chloride in the presence of the cyclam-glyoxal nucleophile. Divalent Mn, Fe, Co, Ni, Cu, and Zn complexes were synthesized and structurally characterized by X-ray crystallography. **PyMeEBC** binds each metal ion in a *cis*-V configuration of the cyclam ring, with the chelated pyridine nitrogen bound to each metal ion, and a chloro ligand occupying the sixth coordination site in all but the 5-coordinate Cu²⁺ complex. Solid state magnetic moment and acetonitrile solution electronic spectroscopy experiments revealed high spin, octahedral, divalent metal complexes in all cases, again with the exception of the 5-coordinate Cu²⁺ complex. Electrochemical studies under an inert atmosphere and in acetonitrile revealed reversible access to

multiple oxidation states, a prerequisite for successful oxidation catalysis, in most cases. In particular, Mn(PyMeEBC)Cl⁺ was stabilized in Mn⁺/Mn²⁺/Mn³⁺/Mn⁴⁺ oxidation states. Finally, preliminary screens for oxidation catalysis using H₂O₂ as the oxidant were carried out on the biomimetically important Mn, Fe, and Cu complexes and showed promising results, particularly for Mn(PyMeEBC)Cl⁺, in the oxidation of thianisole and hydrogen atom abstraction of 1,4-cyclohexadiene. Importantly, Mn(PyMeEBC)Cl⁺ demonstrates powerful, yet selective oxidation reactivity that may lead to improved applications where the Mn(Me₂EBC)Cl₂ catalyst may be too reactive, such as in laundry bleaching. Surprisingly, the copper(II) complex is actually destabilized towards acid decomplexation by the addition of the pyridine pendant arm compared to the parent Me₂EBC complex, which may be a result of a strained structure. Future work will include expanding the range of oxidation reactions possible with this catalyst and determination of its oxidation catalysis mechanisms.

Supporting Information. Detailed crystallographic data. This material is available free of charge via the Internet at <http://pubs.acs.org>.

AUTHOR INFORMATION

Corresponding Author

Timothy J. Hubin, tim.hubin@swosu.edu; Guochuan Yin, gyin@hust.edu.cn; Timothy J.

Prior, T.Prior@hull.ac.uk

Funding Sources

TJH acknowledges Southwestern Oklahoma State University for internal funding through a Proposal Development Award. TJH acknowledges the Donors of the American Chemical Society Petroleum Research Fund; Health Research award for project number HR13-157, from

the Oklahoma Center for the Advancement of Science and Technology; and Grant Number P20RR016478 from the National Center for Research Resources (NCRR), a component of the National Institutes of Health (NIH) for partial support of this research. TJH also acknowledges the Henry Dreyfus Teacher-Scholar Awards Program for support of this work. GY acknowledges support from the National Natural Science Foundation of China (NSFC No. 21273086).

REFERENCES

- [1] T. J. Hubin, J. M. McCormick, S. R. Collinson, M. Buchalova, C. M. Perkins, N. W. Alcock, P. K. Kahol, A. Raghunathan and D. H. Busch, *J. Am. Chem. Soc.*, vol. 122, pp. 2512-2522, 2000.
- [2] T. J. Hubin, J. M. McCormick, N. W. Alcock and D. H. Busch, *Inorg. Chem.*, vol. 40, pp. 435-444, 2001.
- [3] T. J. Hubin, J. M. McCormick, S. R. Collinson, N. W. Alcock, H. J. Clase and D. H. Busch, *Inorg. Chim. Acta*, vol. 346, pp. 76-86, 2003.
- [4] T. J. Hubin, *Coord. Chem. Rev.*, vol. 241, pp. 27-46, 2003.
- [5] G. Yin, M. Buchalova, A. M. Danby, C. M. Perkins, D. Kitko, J. D. Carter, W. M. Scheper and D. H. Busch, *J. Am. Chem. Soc.*, vol. 127, pp. 17170-17171, 2005.
- [6] G. Yin, A. M. Danby, D. Kitko, J. D. Carter, W. M. Scheper and D. H. Busch, *Inorg. Chem.*, vol. 46, pp. 2173-2180, 2007.
- [7] G. Yin, A. M. Danby, D. Kitko, J. D. Carter, W. M. Scheper and D. H. Busch, *J. Am. Chem. Soc.*, vol. 130, pp. 16245-16253, 2008.
- [8] S. Chattopadhyay, R. A. Geiger, G. Yin, D. H. Busch and T. A. Jackson, *Inorg. Chem.*, vol. 49, pp. 7530-7535, 2010.
- [9] S. Shi, Y. Wang, A. Xu, H. Wang, D. Zhu, S. B. Roy, T. A. Jackson, D. H. Busch and G. Yin, *Angew. Chem. Int. Ed.*, vol. 50, pp. 7321-7324, 2011.
- [10] Y. Wang, S. Shi, H. Wang, D. Zhu and G. Yin, *Chem. Commun.*, vol. 48, pp. 7832-7834, 2012.

- [11] Y. Wang, J. Sheng, S. Shi, D. Zhu and G. Yin, *J. Phys. Chem. C*, vol. 116, pp. 13231-13239, 2012.
- [12] Y. Wang, S. Shi, D. Zhu and G. Yin, *Dalton Trans.*, vol. 41, pp. 2612-2619, 2012.
- [13] L. Dong, Y. Wang, Y. Lu, Z. Chen, F. Mei, H. Xiong and G. Yin, *Inorg. Chem.*, vol. 52, pp. 5418-5427, 2013.
- [14] G. Yin, *Acc. Chem. Res.*, vol. 46, pp. 483-492, 2013.
- [15] G. R. Weisman, M. E. Rogers, E. H. Wong, J. P. Jasinski and E. S. Paight, *J. Am. Chem. Soc.*, vol. 112, pp. 8604-8605, 1990.
- [16] D. H. Busch, S. R. Collinson, T. J. Hubin, C. M. Perkins, R. Labeque, B. K. Williams, J. P. Johnston, D. J. Kitko and J. C. T. R. Berkett-St. Laurent, "Bleach Compositions". US Patent 6,218,351, 17 April 2001.
- [17] D. H. Busch, S. R. Collinson, T. J. Hubin, C. M. Perkins, R. Labeque, B. K. Williams, J. P. Johnston, D. J. Kitko, J. C. T. R. Berkett-St. Laurent and M. E. Burns, "Bleach Compositions". US Patent 6,387,862, 14 May 2002.
- [18] D. H. Busch, S. R. Collinson, T. J. Hubin, C. M. Perkins, R. Labeque, B. K. Williams, J. P. Johnston, D. J. Kitko, J. C. T. R. Berkett-St. Laurent and M. E. Burns, "Bleach Compositions". US Patent 6,606,015, 19 August 2003.
- [19] D. H. Busch, S. R. Collinson and T. J. Hubin, "Catalysts and methods for catalytic oxidation". US Patent 6,906,189, 14 June 2005.
- [20] D. H. Busch, S. R. Collinson, T. J. Hubin, C. M. Perkins, R. Labeque, B. K. Williams, J. P. Johnston, D. J. Kitko and J. C. T. R. Berkett-St. Laurent, "Bleach Compositions". US Patent 7,125,832, 24 October 2006.
- [21] Y. Feng, J. England and L. J. Que, *ACS Catal.*, vol. 1, pp. 1035-1042, 2011.
- [22] G. Yin, A. M. Danby, V. Day, S. B. Roy, J. Carter, W. M. Scheper and D. H. Busch, *J. Coord. Chem.*, vol. 64, pp. 4-17, 2011.
- [23] G. Yin, S. B. Roy, A. M. Danby, V. Day, J. Carter, W. M. Scheper and D. H. Busch, *J. Incl. Phenom. Macrocycl. Chem.*, vol. 71, pp. 311-318, 2011.
- [24] A. Thibon, J. England, M. Martinho, V. G. J. Young, J. R. Frisch, R. Guillot, J.-J. Girerd, E. Munck, L. J. Que and F. Banse, *Angew. Chem. Int. Ed.*, vol. 47, pp. 7064-7067, 2008.
- [25] N. W. Alcock, K. P. Balakrishnan and P. Moore, *J. Chem. Soc., Dalton Trans.*, pp. 1743-1745, 1986.

- [26] E. Asato, S. Hashimoto, N. Matsumoto and S. Kida, *J. Chem. Soc., Dalton Trans.*, pp. 1741-1746, 1990.
- [27] G. Vuckovic, E. Asato, N. Matsumoto and S. Kida, *Inorg. Chim. Acta*, vol. 171, pp. 45-52, 1990.
- [28] G. Royal, V. Dahaoui-Gindrey, S. Dahaoui, A. Tabard, R. Guilard, P. Pullumbi and C. Lecomte, *Eur. J. Org. Chem.*, pp. 1971-1975, 1998.
- [29] C. Bucher, G. Royal, J.-M. Barbe and R. Guilard, *Tetrahedron Lett.*, vol. 40, pp. 2315-2318, 1999.
- [30] A. E. Goeta, J. A. K. Howard, D. Maffeo, H. Puschmann, J. A. G. Williams and D. S. Yufit, *J. Chem. Soc., Dalton Trans.*, pp. 1873-1880, 2000.
- [31] A. S. Batsanov, A. E. Goeta, J. A. K. Howard, D. Maffeo, H. Puschmann and J. A. G. Williams, *Polyhedron*, vol. 20, pp. 981-986, 2001.
- [32] S. El Ghachtouli, C. Cadiou, I. Dechamps-Olivier, F. Chuburu, M. Aplincourt and T. Roisnel, *Eur. J. Inorg. Chem.*, pp. 3472-3481, 2006.
- [33] S. El Ghachtouli, C. Cadiou, I. Dechamps-Olivier, F. Chuburu, M. Aplincourt, V. Patinec, M. Le Baccon, H. Handel and T. Roisnel, *New J. Chem.*, vol. 30, pp. 392-398, 2006.
- [34] J. Narayanan, A. Solano-Peralta, V. M. Ugalde-Salvidar, R. Escudero, H. Hopfl and M. E. Sosa-Torres, *Inorg. Chim. Acta*, vol. 361, pp. 2747-2758, 2008.
- [35] J.-F. Morfin, R. Tripier, M. Le Baccon and H. Handel, *Polyhedron*, vol. 28, pp. 3691-3698, 2009.
- [36] N. Bernier, J. Costa, R. Delgado, V. Felix, G. Royal and R. Tripier, *Dalton Trans.*, vol. 40, pp. 4514-4526, 2011.
- [37] E. K. Barefield, F. Wagner, A. W. Herlinger and A. R. and Dahl, *Inorganic Syntheses*, vol. XVI, pp. 220-225, 1976.
- [38] M. Le Baccon, F. Chuburu, L. Toupet, H. Handel, M. Soibinet, I. Deschamps-Olivier, J.-P. Barbier and M. Aplincourt, *New J. Chem.*, vol. 25, pp. 1168-1174, 2001.
- [39] T. J. Hubin, J. M. McCormick, N. W. Alcock, H. J. Clase and D. H. Busch, *Inorg. Chem.*, vol. 38, pp. 4435-4446, 1999.
- [40] *X-Area v 1.64*, Darmstadt: STOE & Cie GmbH, 2012.
- [41] G. Sheldrick, *Acta Crystallogr. Sect. A: Found. Crystallogr.*, vol. 64, pp. 112-122, 2008.

- [42] G. R. Weisman, E. H. Wong, D. C. Hill, M. E. Rogers, D. P. Reed and J. C. Calabrese, *Chem. Commun.*, pp. 947-948, 1996.
- [43] E. H. Wong, G. R. Weisman, D. C. Hill, D. P. Reed, M. E. Rogers, J. P. Condon, M. A. Fagan, J. C. Calabrese, K.-C. Lam, I. A. Guzei and A. L. Rheingold, "J. Am. Chem. Soc.," vol. 122, 2000.
- [44] M. F. Almassio, M. N. Sarimbali and R. O. Garay, *Designed Monomers and Polymers*, vol. 8, pp. 287-296, 2005.
- [45] S. Rojas-Limas, N. Farfan, R. Santillan, D. Castillo, M. E. Sosa-Torres and H. Hopfl, *Tetrahedron*, vol. 56, pp. 6427-6433, 2000.
- [46] F. El Hajj, G. Sebki, V. Patinec, M. Marchivie, S. Triki, H. Handel, S. Yefsah, R. Tripier, C. J. Gomez-Garcia and E. Coronado, *Inorg. Chem.*, vol. 48, pp. 10416-10423, 2009.
- [47] S. Fuzerova, J. Kotek, I. Cisarova, P. Hermann, K. Binnemans and I. Lukes, *Dalton Trans.*, pp. 2908-2915, 2005.
- [48] J. L. P. Kotek, P. Hermann, I. Cisarova, I. Lukes, T. Godula, I. Svobodova, P. Taborsky and J. Havel, *Chem. Eur. J.*, vol. 9, pp. 233-248, 2003.
- [49] X. Sun, M. Wuest, Z. Kovacs, A. D. Sherry, R. Motekaitis, Z. Wang, A. E. Martell, M. J. Welch and C. J. Anderson, *J. Biol. Inorg. Chem.*, vol. 8, pp. 217-225, 2003.
- [50] I. Svobodova, J. Havlickova, J. Plutnar, J. Plutnar, P. Lubal, J. Kotek and P. Hermann, *Eur. J. Inorg. Chem.*, pp. 3577-3592, 2009.
- [51] T. J. Hubin, N. W. Alcock, H. J. Clase, L. L. Seib and D. H. Busch, *Inorg. Chim. Acta*, vol. 337, pp. 91-102, 2002.
- [52] A. W. Addison, T. N. Rao, J. Reedijk, J. van Rijn and G. C. Verschoor, *J. Chem. Soc., Dalton Trans.*, pp. 1349-1356, 1984.
- [53] A. Bondi, *J. Phys. Chem.*, vol. 68, pp. 441-451, 1964.
- [54] C. R. Groom and F. H. Allen, *Angew. Chem. Int. Ed.*, vol. 53, pp. 662-671, 2014.
- [55] T. J. Hubin, "unpublished data," 2014.
- [56] T. J. Hubin, N. W. Alcock, H. J. Clase and D. H. Busch, *Supramolec. Chem.*, vol. 13, pp. 261-276, 2001.
- [57] K. Burger, *Coordination Chemistry: Experimental Methods*, London: Butterworth, 1973.
- [58] A. B. P. (Lever), *Inorganic Electronic Spectroscopy*, 2nd ed., Amsterdam: Elsevier, 1984.

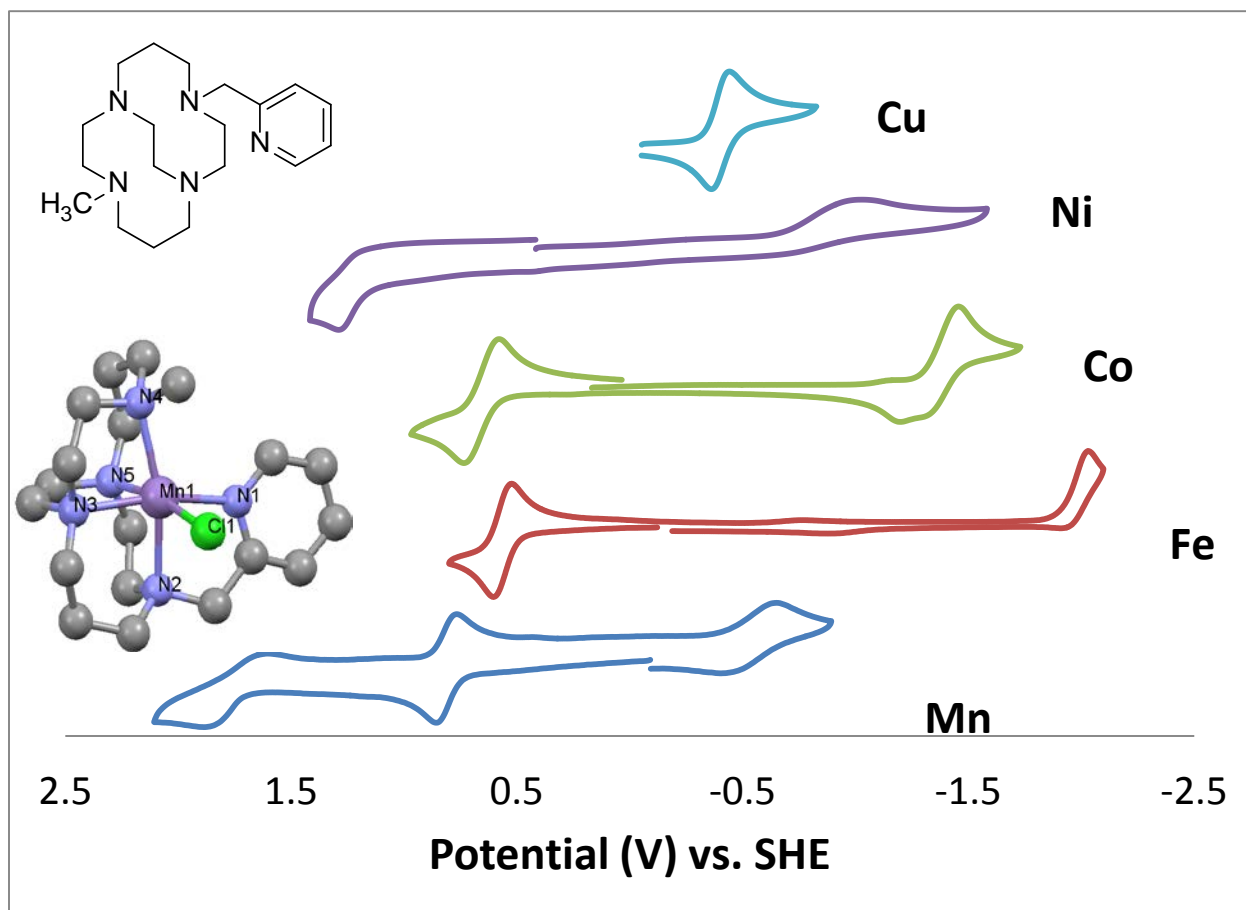
- [59] R. S. Drago, *Physical Methods for Chemists*, 2nd ed., Ft. Worth: Saunders College Publishing-Harcourt Brace Jovanovich, 1992.
- [60] T. J. Hubin, N. W. Alcock, M. D. Morton and D. H. Busch, *Inorg. Chim. Acta*, vol. 348, pp. 33-40, 2003.
- [61] T. J. Hubin, N. W. Alcock and D. H. Busch, *Acta Cryst.*, vol. C56, pp. 37-39, 2000.
- [62] J. M. Mayer, *Acc. Chem. Res.*, vol. 31, pp. 441-450, 1998.
- [63] M. C. Carreno, *Chem. Rev.*, vol. 95, pp. 1717-1760, 1995.
- [64] M. Ghorbanloo, M. Jaworska, P. Paluch, G.-D. Li and L.-J. Zhou, *Transition Met. Chem.*, vol. 38, pp. 511-521, 2013.
- [65] X.-T. Zhou and H.-B. Ji, *Catalysis Commun.*, vol. 53, pp. 29-32, 2014.
- [66] H. So, Y. J. Park, K.-B. Cho, Y.-M. Lee, M.-S. Seo, J. Cho, R. Sarang and W. Nam, *J. Am. Chem. Soc.*, vol. 136, pp. 12229-12232, 2014.
- [67] J. Brinksma, R. La Crois, B. L. Feringa, M. I. Donnoli and C. Rosini, *Tetrahedron Lett.*, vol. 42, pp. 4049-4052, 2001.
- [68] G. B. Shul'pin, G. Suss-Fink and L. S. Shul'pina, *J. Molec. Catal. A*, vol. 170, pp. 17-34, 2001.
- [69] J. R. Lindsay Smith, B. C. Gilbert, A. Mairata i Payeras, J. Murray, T. R. Lowdon, J. Oakes, R. Pons i Prats and P. H. Walton, *J. Molec. Catal. A*, vol. 251, pp. 114-122, 2006.
- [70] T. J. Hubin, J. M. McCormick, S. R. Collinson, N. W. Alcock and D. H. Busch, *Chem. Commun.*, pp. 1675-1676, 1998.
- [71] K. S. Woodin, K. J. Heroux, C. A. Boswell, E. H. Wong, G. R. Weisman, W. Niu, S. A. Tomellini, C. J. Anderson, L. N. Zakharov and A. L. Rheingold, *Eur. J. Inorg. Chem.*, vol. 7, pp. 4829-4833, 2005.
- [72] K. J. Heroux, K. S. Woodin, D. J. Tranchemontagne, P. C. B. Widger, E. Southwick, E. H. Wong, G. R. Weisman, S. A. Tomellini, T. J. Wadas, C. J. Anderson, S. Kassel, J. A. Golen and A. L. Rheingold, *Dalton Trans.*, pp. 2150-2162, 2007.
- [73] C. J. Anderson, T. J. Wadas, E. H. Wong and G. R. Weisman, *Quart. J. Nuc. Med. Mol. Imag.*, vol. 52, pp. 185-192, 2008.
- [74] A. Y. Odendaal, A. L. Fiamengo, R. Ferdani, T. J. Wadas, D. C. Hill, Y. Peng, K. J. Heroux, J. A. Golen, A. L. Rheingold, C. J. Anderson, G. R. Weisman and E. H. Wong, *Inorg. Chem.*, vol. 50, pp. 3078-3086, 2011.

- [75] D. H. Busch, *Chem. Rev.*, vol. 93, pp. 847-860, 1993.
- [76] X. Sun, M. Wuest, G. R. Weisman, E. H. Wong, D. P. Reed, C. A. Boswell, R. Motekaitis, A. E. Martell, M. J. Welch and C. J. Anderson, "J. Med. Chem.," vol. 45, 2002.
- [77] J. Lichty, S. M. Allen, A. I. Grillo, S. J. Archibald and T. J. Hubin, *Inorg. Chim. Acta*, pp. 615-618, 2004 (357).
- [78] J. E. Sprague, Y. Peng, X. Sun, G. R. Weisman, E. H. Wong, S. Achilefu and C. J. Anderson, *Clinical Cancer Res*, vol. 10, pp. 8674-8682, 2004.
- [79] J. E. Sprague, Y. Peng, A. L. Fiamengo, K. S. Woodin, E. A. Southwick, G. R. Wiesman, E. H. Wong, J. A. Golen, A. L. Rheingold and C. J. Anderson, *J. Med. Chem.*, vol. 50, pp. 2527-2535, 2007.
- [80] D. J. Stigers, R. Ferdani, G. R. Weisman, E. H. Wong, C. J. Anderson, J. A. Golen, C. Moore and A. L. Rheingold, *Dalton Trans.*, vol. 39, pp. 1699-1701, 2010.
- [81] D. Zeng, Q. Ouyang, Z. Cai, X.-Q. Xie and C. J. Anderson, *Chem. Commun.*, vol. 50, pp. 43-45, 2014.
- [82] C. A. Boswell, X. Sun, W. Niu, G. R. Weisman, E. H. Wong, A. L. Rheingold and C. J. Anderson, *J. Med. Chem.*, vol. 47, pp. 1465-1474, 2004.
- [83] C. A. Boswell, P. McQuade, G. R. Weisman, E. H. Wong and C. J. Anderson, *Nucl. Med. Biol.*, vol. 32, pp. 29-38, 2005.
- [84] J. D. Silversides, B. P. Burke and S. J. Archibald, *C. R. Chimie*, vol. 16, pp. 524-530, 2013.
- [85] J. D. Silversides, R. Smith and S. J. Archibald, *Dalton Trans.*, vol. 40, pp. 6289-6297, 2011.
- [86] C. A. Boswell, C. A. S. Regino, K. E. Baidoo, K. J. Wong, A. Bumb, H. Xu, D. E. Milenic, J. A. Kelley, C. C. Lai and M. W. Brechbiel, *Bionconjugate Chem.*, vol. 19, pp. 1476-1484, 2008.
- [87] M. Persson, M. Hosseini, J. Madsen, T. J. D. Jorgensen, K. J. Jensen, A. Kjaer and M. Ploug, *Theranostics*, vol. 3, pp. 618-632, 2013.
- [88] L. M. P. Lima, Z. Halime, R. Marion, N. Camus, R. Delgado, Platas-Iglesias, C. and R. Tripier, *Inorg. Chem.*, vol. 53, pp. 5269-5279, 2014.
- [89] A. Khan, J. Greenman and S. J. Archibald, *Curr. med. Chem.*, vol. 14, pp. 2257-2277, 2007.
- [90] E. De Clercq, *Curr. Opin. Pharmacol.*, vol. 10, pp. 507-515, 2010.

- [91] J. A. Este, C. Cabrera, E. De Clercq, S. Struyf, J. Van Damme, G. Bridger, R. T. Skerlj, M. J. Abrams, G. Henson, A. Gutierrez, B. Clotet and D. Schols, *Mol. Pharmacol.*, vol. 55, pp. 67-73, 1999.
- [92] S. Hatse, K. Princen, L. O. Gerlach, G. Bridger, G. Henson, E. De Clercq, T. W. Schwartz and D. Schols, *Mol. Pharmacol.*, vol. 60, pp. 164-173, 2001.
- [93] E. De Clercq, *Nat. Rev. Drug Discovery*, vol. 2, pp. 581-587, 2003.
- [94] G. A. Donzella, D. Schols, S. W. Lin, J. A. Este, K. A. Nagashima, P. J. Maddon, G. P. Allaway, T. P. Sakmar, G. Henson, E. De Clercq and J. P. Moore, *Nat. Med.*, vol. 4, pp. 72-77, 1998.
- [95] W. C. Liles, H. E. Broxmeyer, E. Rodger, B. Wood, K. Hubel, S. Cooper, G. Hancoc, G. Bridger, G. W. Henson, G. Calandra and D. C. Dale, *Blood*, vol. 102, pp. 2728-2730, 2003.
- [96] D. Schols, *Antiviral Res.*, vol. 71, pp. 216-226, 2006.
- [97] E. T. Roussos, J. S. Candeelis and A. Patsialou, *Nat. Rev. Cancer*, vol. 11, pp. 573-587, 2011.
- [98] G. C. Valks, G. McRobbie, E. A. Lewis, T. J. Hubin, T. M. Hunter, P. J. Sadler, C. Pannecouque, E. De Clercq and S. J. Archibald, "J. Med. Chem.," vol. 49, 2006.
- [99] A. Khan, G. Nicholson, J. Greenman, L. Madden, G. McRobbie, C. Pannecouque, E. De Clercq, J. D. Silversides, R. Ullom, D. L. Maples, R. D. Maples, T. J. Hubin and S. J. Archibald, "J. Am. Chem. Soc.," vol. 131, 2009.
- [100] R. Smith, D. Huskens, R. E. Mewis, C. D. Garcia, A. N. Cain, T. N. Carder Freeman, C. Pannecouque, E. De Clercq, D. Schols, T. J. Hubin and S. J. Archibald, "Dalton Trans.," 2012.
- [101] J. C. Timmons and T. J. Hubin, *Coord. Chem. Rev.*, vol. 254, pp. 1661-1685, 2010.
- [102] S. Hatse, K. Princen, E. De Clercq, M. M. Rosenkilde, T. W. Schwartz, P. E. Hernandez-Abad, Skerlj, R. T., G. J. Bridger and D. Schols, *Biochem. Pharmacol.*, vol. 70, pp. 752-761, 2005.
- [103] M. M. Rosenkilde, L.-O. Gerlach, S. Hatse, R. T. Skerlj, D. Schols, G. J. Bridger and T. W. Schwartz, *J. Biol. Chem.*, vol. 282, pp. 27354-27365, 2007.
- [104] V. Bodart, V. Anastassov, M. C. Darkes, S. R. Idzan, J. Labrecque, G. Lau, R. M. Mosi, K. S. Neff, K. L. Nelson, M. C. Ruzek, K. Patel, Z. Santucci, R. Scarborough, R. S. Y. Wong, G. J. Bridger, R. T. MacFarland and S. P. Fricker, *Biochem. Pharmacol.*, vol. 78, pp. 993-1000, 2009.

- [105] G. J. Bridger, R. T. Skerlj, P. E. Hernandez-Abad, D. E. Bogucki, Z. Wang, Y. Zhou, S. Nan, E. M. Boehringer, T. Wilson, J. Crawford, M. Metz, S. Hatse, K. Princen, E. De Clercq and D. Schols, *J. Med. Chem.*, vol. 53, pp. 1250-1260, 2010.
- [106] R. A. De Silva, K. Peyre, M. Pullambhatla, J. J. Fox, M. G. Pomper and S. Nimmagadda, *J. Nucl. Med.*, vol. 52, pp. 986-993, 2011.
- [107] X. Ling, E. Spaeth, Y. Chen, Y. Shi, W. Zhang, W. Schober, N. J. Hail, M. Konopleva and M. Andreef, *PLOS One*, vol. 8, p. e58426, 2013.
- [108] L. E. Woodard, R. A. De Silva, B. Benham Azad, A. Lisok, M. Pullambhatla, W. G. Lesniak, R. C. Mease, M. G. Pomper and S. Nimmagadda, *Nucl. Med. Biol.*, vol. 41, pp. 552-561, 2014.

Table of Contents Graphic and Synopsis



TOC Synopsis: 2-pyridylmethyl pendant armed ethylene cross-bridged cyclam complexes stabilize transition metals in multiple oxidation states, allowing for efficient oxidation catalysis.